Test Plan

Initial optimization and design of a bio-inspired Wave Energy Converter

Awardee: Jim Marson

Awardee point of contact: James Marson

Facility: Sandia National Laboratories

Facility point of contact: Dominic Forbush

Date: 7/10/2025 (RFTS 10)

EXECUTIVE SUMMARY

Existing software tools including Capytaine, wecOptTool, and wecSim were used to examine and perform low-order optimization of the hydrodynamics and power performance of a Marson-type device. The device is a segmented nominally circular float that can be divided along variable radial or azimuthal intervals, resulting in configurations suitable for variety of deployment situations (affixed to existing structure vs. free-floating) and requiring a varying number of power-take-offs and power aggregation strategies. The initial objectives of this study were to employ wecOptTool to understand the hydrodynamic power capture potential of different device configurations in a variety of common offshore and nearshore sea-states to identify promising subsets of device configurations, specifically viable numbers of radial and azimuthal sections and overall device size. Once identified, the second aim of this study was to explore low-level models of power-take-off and control strategies for the viable configurations within WEC-Sim: this allowed hydrodynamic and other non-linearities to be included and, after iteration in wecOptTool, arrive at component level models. The goal of this project was not necessarily to converge on an optimal design for each sea state, but to examine trends in performance due to varied design parameters that will help narrow the potential design and market/application space for future, detailed development.

This project had a number of challenges that limited the success of the project. These challenges were primarily due to the challenges in modeling the dynamics of the attenuator WEC directly in WecOptTool. Impedance models were created using WEC-Sim, but these still presented challenges when analyzing in WecOptTool. A final set of batch runs of WEC-Sim simulations provided opportunity for additional analysis. Despite the challenges and limitations of the analysis completed, a number of valuable conclusions could still be made. A floating version of the Marson WEC showed potential as compared to a traditional point absorber of similar dimension, especially for bimodal seas, but efficient PTO design is vital to ensuring success. Further, since the heave modes seemed to dominate the power extraction, it is unlikely that more than 3 floats provides significant benefits. The Marson WEC will also present an opportunity to test and improve the co-design and system identification process for similar WECs involving kinematic chains. Through this project, some valuable design insights regarding the Marson WEC have been achieved, and relevant design challenges have been made clear for the modeling team to improve upon.

1 Introduction to the project

Through TEAMER, Jim Marson (Marson) worked with Sandia National Laboratories (Sandia) to produce a set of numerical models of the Marson device, a bio-inspired WEC archetype with potentially numerous functional geometries/configurations, to identify a promising set of archetypes in realistic sea-states for further future study. Open-source tools were utilized in all steps of the analysis so that future research on the device can be accessible.

2 Roles and Responsibilities of Project Participants

2.1 Applicant Responsibilities and Tasks Performed

Marson provided Sandia with the proposed WEC concept, rough geometries, and power take off designs that were considered for analysis. In collaboration with Sandia, Marson down-selected promising configurations for realistic applications of interest and highlighted a few for future study. Marson ultimately desires to hand off this technology for exploration and development in the public domain.

2.2 Network Facility Responsibilities and Tasks Performed

Sandia led the numerical modeling and analysis efforts. Sandia parameterized device geometry in a manner suitable for analysis in the boundary-element-method modeling tool Capytaine and wecOptTool. Sandia constructed the wecOptTool model to identify promising device configurations, and, in collaboration with Marson, selected a few for non-linear time-domain analysis in WEC-Sim. Sandia constructed the WEC-Sim model, including power-take-off components, and analyze power, displacement, and structural load data. Sandia produced documentation outlining the completed analysis, justification for the selection of viable geometries, and significant findings in a final report.

3 Project Objectives

The objective of this project was to perform preliminary numerical analysis of the Marson device (Figure 1) to advise the most promising device configurations for realistic sea-states and applications. This process suggested particular variants of the device for future detailed analysis/design, beyond the scope of this award. A "promising" device hes been determined by both qualitative and quantitative measures. Qualitatively, minimizing device complexity by reducing the number of floats, PTOs, and linkages was desirable. Quantitatively desirable metrics include maximizing power capture per device size and limiting structural loads to tractable limits. Although an explicit examination of device cost was beyond the scope of proposed work, the combination of these metrics is likely to reduce overall device cost.

Marson wishes to utilize this device as an open-source design to further marine renewable energy interests industry-wide.

3.1 BEM Modeling

Because this device geometry was readily parameterizable and can be modeled with reasonable accuracy via boundary-element-methods (BEM), it is ideal for early-stage optimization and co-design within WecOptTool (Figure 4) for a variety of configurations. WecOptTool is configured by default to utilize Capytaine, an open-source BEM code. Two approaches to



Figure 1: A rendering of one possible device configuration. The device can vary from a circular cross section to this nearly-linear attenuator by varying the number, size, and layout of float sections. Power is extracted through the relative pitching motion between float sections. Optimizing the number, layout, and size of radial and azimuthal sections was a key objective of this work. The work can model affixing the device to an existing floating or fixed structure by considering the inner-most float as connected to this structure.

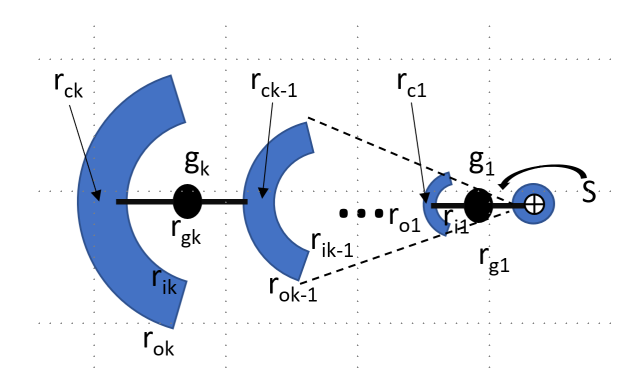


Figure 2: An example of a parameterization of device geometry suitable for wecOptTool that can facilitate the analysis of a wide variety of shapes. Shown from a top view, the device consists of k floats and k generators, with the identifying numbers increasing outwards from the central platform. One such segment of these elements is shown, but additional groups arrayed circularly around the central platform, can be analyzed similarly. Alternatively, straight floats can also be considered.

BEM modeling the various possible geometries of this device in BEM were apparent: multiple body and generalized body mode approaches. Both were investigated, with preference given to the method that yielded consistently reasonable results (i.e., minimal singularities). A generalized geometry parameterization is shown in Figure 2 for each body, and both multiple body and generalized body mode methods are shown as schematics in Figure 3.

The draft of each float was also considered at this phase. Though this has implications on the weight of each float, the weight was not specified at this point. Additionally, straight floats were considered for simplicity.

3.2 WecOptTool Modeling

As shown in Figure 4, BEM modeling and results are part of the iterative WecOptTool loop, but additionally the kinematic relationships between WEC and PTO motions had to be parameterized. For this device, the PTO generally moves due to relative displacements be-

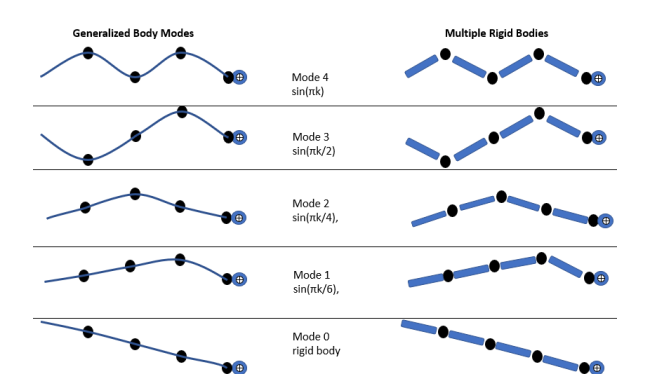


Figure 3: Two proposed BEM modeling approaches for k floats, (shown with k = 4). The representation of k rigid bodies is shown at right, and at left is an approximation of the rigid body system using a single, flexible body with k additional generalized body modes.

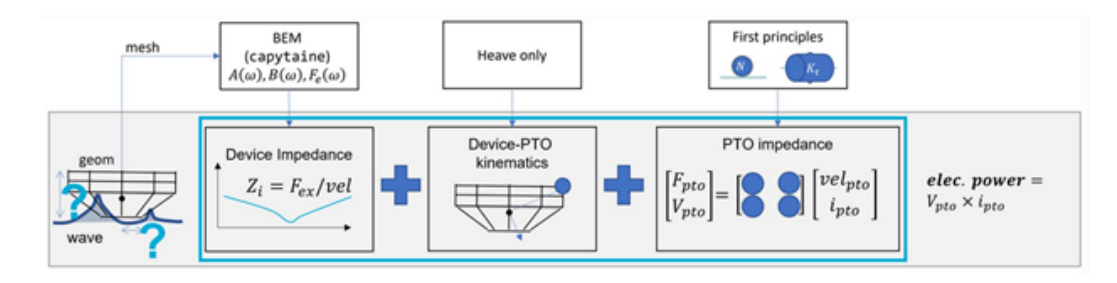


Figure 4: A schematic of the wecOptTool co-optimization procedure. By parameterizing device geometry and describing the kinematic relationships between prime movers and PTO components, the device geometry, PTO parameters, and controller can be simultaneously optimized for a given sea-state. Comparing the performance of various morphologies can suggest promising configurations and provide initial design specifications for PTO and controller components.

tween adjacent bodies. For small displacements, the angular displacement of the k generator is defined by relative heave displacements of adjacent bodies.

$$\theta_{gk} = N_k \left(\arctan\left(\frac{x_{3,k}}{r_{ck} - r_{gk}}\right) + \arctan\left(\frac{x_{3,k-1}}{r_{gk} - r_{ck-1}}\right) \right)$$
 (1)

which, again assuming small displacements, linearizes to

$$\theta_{gk} = N_k \left(\frac{x_{3,k}}{r_{ck} - r_{gk}} + \frac{x_{3,k-1}}{r_{gk} - r_{ck-1}} \right)$$
 (2)

where parameters are tabulated in Table 2. Note that for larger displacements, surge motions also cause generator angular displacement and that float pitch is not independent from heave and surge as each body is constrained by the fixed radius between it and the generator. Represented by BEM coefficients with kinematics described by Eq 2, initial optimizations are expected to favor geometries offering substantial relative heave displacements. To understand the effect of the various parameters on WEC performance, illuminate trends in power capture and loads, and inform useful initial guesses for optimization, the first WecOptTool runs investigated batches of fixed geometries.

For a direct-drive generator system, the power-take-off impedance was parameterized by the motor constant K_t , the winding resistance R_w , the generator inertia J_g , mechanical

Table 1: Range of sea-states for investigation and targeted for optimization

| | Significant Heights (m) | Peak Periods (s) | | |
|--------|-------------------------|------------------|--|--|
| Range | 0.5 - 5 | 2-17 | | |
| Target | 1-3 (PacWave) | 7-11 (PacWave) | | |

damping B_g , drivetrain stiffness K_g , and the winding inductance L_w . See, for example [1], [2], and [3]. While all can be optimization parameters, it was only useful to consider realistic, non-zero values of R_w and B_g as optimization otherwise minimized this parasitic loss. Notably, a parameterization at this level of fidelity was conducive to time-domain WEC-Sim modeling at a simple component level.

Beginning at the WecOptTool stage, and continuing into WEC-Sim modeling, sea-states prevalent at PacWave for all geometries were targeted, but a broad range of sea states were investigated to understand the trends in optimal designs. The most promising configurations for the floating and structure-fixed WEC were investigated in WEC-Sim for the targeted sea-states (at a minimum). The most promising configurations maximize the power per generator number, power per float volume, and minimize PTO and structural loads. ¹

3.3 WEC-SIM MODELING

A higher fidelity, time-domain model was then be developed for promising configurations in WEC-Sim: which, using system identification techniques [4], improves the WecOptTool representation iteratively. Ultimately, two or more promising configurations were modeled in WEC-Sim to the level of simple components/controllers, and time-domain analysis estimated power capture, loads, and dynamics to suggest areas of future application or further study. While WEC-Sim relied similarly on BEM coefficients, the realistic non-linear kinematics and dynamics can be directly represented: a key validation of WecOptTool suggested geometries. Particularly, the nonlinear kinematics (which are linearized through system identification) were fully resolved in WEC-Sim.

3.3.1 Mooring Systems

WEC-Sim modeling facilitated the investigation of possible different mooring systems, and, if their effect on system dynamics were significant, allowed their incorporation via system identification into the WecOptTool device model. The following systems will be considered.

- 1. Fixed platform. In this case, the central body is assumed to be attached to another structure (i.e., bridge, pylon, pier) that is fixed.
- 2. Single-point pre-tensioned cable to the central body. For a free-floating WEC, this exerts large mooring force on the central body in the heave direction and smaller mooring force in the surge direction that increases with increasing surge displacement.
- 3. Multi-point caternary to the central body. For a free-floating WEC, this can exert a moderate mooring force in the heave, surge, and pitch directions.

¹The optimizer similarly attempts to minimize any parasitic damping on the float side of the PTO: the extent to which these losses can/should be minimized is ultimately a question of the cost to reduce each term at the optimal gear ratio(s). This requires a component-level cost (in \$) model that is beyond the scope of the planned work.

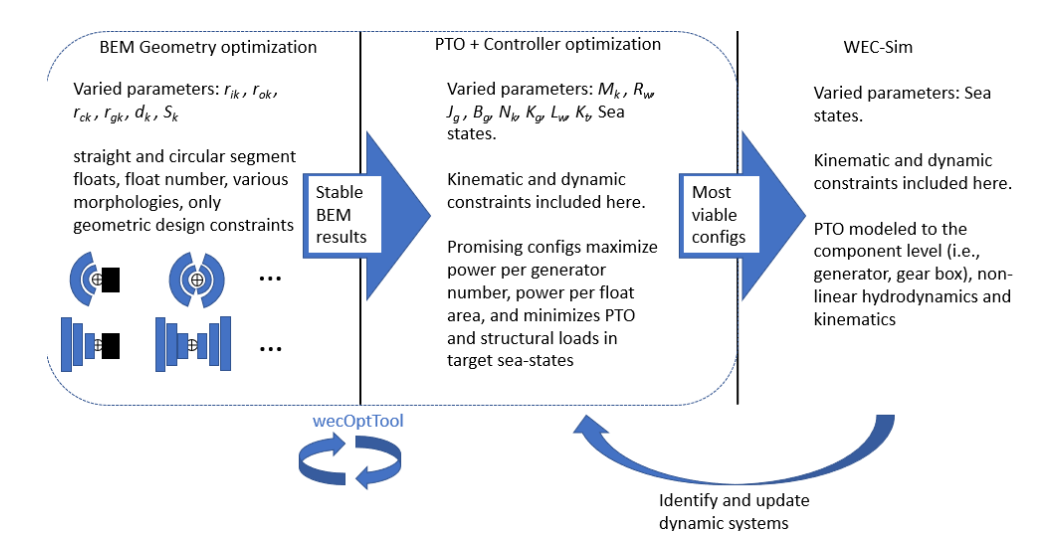


Figure 5: An overview of the proposed workflow including the parameters varied at each stage of modeling. WecOptTool performs simultaneous optimization of buoy geometry, PTO, and control, but relies on a stable BEM solution.

A detailed design of these mooring systems is beyond the scope of this project, however an understanding of the loads and displacements experienced by the WEC in various configurations and with various moorings has been useful for future mooring design.

3.4 Workflow Overview

The workflow is summarized in Figure 5. Note that BEM is included within the WecOpt-Tool iteration, however, the stability and reliability of BEM results was ensured prior to iteration within the optimization loop, and thus it is presented sequentially. The BEM approach for each unique WEC morphology (i.e., circular vs. straight floats, structure-fixed vs. free-floating) was considered individually, and each unique WEC morphology required an additional run of WecOptTool. WecOptTool simultaneously optimizes geometry, PTO, and controller in specified sea-states to a user-defined cost function. Specifically, the cost function(s) maximized total electrical power capture per number of generators, electrical power capture per float volume, while minimizing PTO and structural loads in target sea-states.

The system models used initially by WecOptTool were refined using the WEC-Sim model by identifying new system models from WEC-Sim, which include the effects of non-linearities in hydrodynamics and PTO components. This procedure allowed for iterated to make sure that the suggested optima are representative of the system dynamics at the highest available level of fidelity.

4 TEST FACILITY, EQUIPMENT, SOFTWARE, AND TECHNICAL EXPERTISE

- \bullet Physical equipment, hardware, instrumentation and other capabilities essential to achieving project objectives N/A
- Simulation or data analysis software utilized This project relied on Capytaine, We-cOptTool, and WEC-Sim.

- Critical personnel expertise utilized to achieve the project objectives
 - Dominic Forbush: Dr. Dominic Forbush is a senior research and development engineer in the Water Power Technologies Program at Sandia National Laboratories. Dominic's research focuses on the control, modeling, and the development of innovative solutions for wave energy converters (WECs). Particularly, Dominic is involved in developing and supporting open-source WEC modeling tools, wave tank testing of WEC devices and control approaches, and the application structured innovation techniques to the wave energy space. Dominic has a bachelor's, master's, and doctorate all in mechanical engineering from the University of Washington, where his graduate work focused on the control of cross-flow hydrokinetic turbines.
 - Jeff Grasberger: Jeff Grasberger is a research and development engineer at Sandia National Laboratories and a developer of WEC-Sim and WecOptTool.

5 Test or Analysis Article Description

The WEC concept is one of highly variable, though readily parameterizable, geometry that is suitable across its potential configurations for deployment as an independent floating platform, part of a large array of similar devices, or attached to existing static or floating offshore structures.

In this way, the geometric concept can range from an attentuator (for instance Figure 2, with additional elements mirrored across the right side).

A variety of device configurations were examined in wecOptTool, with the most promising subset examined further with a refined time-domain WEC-Sim model.

6 Work Plan

Of the proposed 125,000\$ budget at Sandia, the cost breakdown per task is estimated next to the estimated duration.

- 1. Developed a parameterized BEM model for the free-floating circular and semi-circular structure-fixed morphologies according to Figure 2. [Month 1-2, \$35,000]
- 2. Using Marsons' proposed direct-drive PTO morphology, developed kinematic/dynamic equations relating float motions/forces to PTO motions/forces. [Month 1-2 (concurrently with above), \$10,000]
- 3. Imposed kinematic constraints on the float/PTO motion, at a minimum those in Table 2. After investigating unconstrained loads, the sensitivity of the resulting optimal architecture to increasingly restrictive load constraints was investigated. [Month 2, \$10,000]
- 4. Use 1) -3) as inputs to WecOptTool. Sweeping over a broad range of sea-states determined trends in optimal parameters as functions of period and wave height. Investigation took place with sea-states estimated from PacWave information. [Month 3, \$15,000]

Table 2: Parameter and constraint description

| Parameter | Description |
|---|---|
| g_k | The kth generator/motor |
| r_{ik} | The inner radius of the kth float, measured |
| | from origin |
| r_{ok} | The outer radius of the kth float. |
| r_{ck} | The radius at the center of mass of the kth |
| | float. |
| r_{gk} | The distance from origin of the kth generator |
| d_k | The draft of the kth float |
| S_k | Azimuthal sweep angle/length of the kth float. |
| | If an angular sweep, this is constant for all |
| | floats |
| M_k | The static mass of the kth float |
| X_{5k} | The pitch displacement of the kth float |
| X_{3k} | The heave displacement of the kth float |
| X_{1k} | The surge displacement of the kth float |
| N_k | The gear ratio relating generator angular dis- |
| | placement to the angular displacement of con- |
| | nected floating bodies |
| $\bigcup J_{gk}$ | kth generator and PTO inertia |
| B_{gk} | kth PTO mechanical damping |
| K_{gk} | kth PTO mechanical stiffness |
| K_{tk} | Motor constant of the kth generator |
| R_{wk} | Winding resistance of the kth generator |
| L_{wk} | Winding inductance of the kth generator |
| Constraint | ******** |
| $r_{o,k} > r_{c,k} > r_{i,k} > r_{g,k-1}$ | The k-1 generator must be inside the kth float, |
| | which has geometric constraints |
| $\Theta_{gk-1}/N_{k-1} < \Theta_{max,k}$ | A limitation on the stroke of the linkage, with |
| | gear ratio N , between the floats (e.g., the |
| | floats cannot rotate to the point of interfer- |
| | ing with each other). |
| $M_k < \text{displaced volume}$ | Each float must float. |

6.1 Safety 6 WORK PLAN

5. For the morphologies suggested for detailed investigation, a WEC-Sim model was constructed. Quadratic drag was included based upon geometric estimates, non-linear Froude-Krylov forces, kinematic constraints, mooring, and a preliminary model using transfer-function approximation of PTO was employed initially. [Month 3 and 4, \$15,000]

- 6. WEC-Sim models were run, estimates of electrical power capture and loads exerted on floats, connections, and PTOs were developed for investigated sea states for several levels of PTO load constraints [Month 4, \$10,000].
- 7. Using system identification techniques, the device intrinsic impedance model from WEC-Sim was identified (including contributions from mooring and non-linear terms) and run WecOptTool again using this model: repeat 5)-6) for significant differences in suggested parameters. [Month 5, \$5,000].
- 8. WEC-Sim models were updated to include simple component-level representations of the WecOptTool-suggested PTO. Electrical power capture and load estimates were recreated. This component-level model will facilitate future design iterations. [Month 5, \$10,000].
- 9. Findings were summarized in report, emphasizing the relationship between optimal device design parameters and investigated sea-states and PTO force constraints on device power capture and loads. Potential component-level PTO morphologies are suggested. [Month 6, \$10,000]
- 10. A journal article was considered but not pursued at this time. [Month 6, \$5,000]

6.1 SAFETY

N/A - this is a numerical analysis project

6.2 Contingency Plans

This tool development relied upon several already-existing packages being readily adaptable to the necessary modifications, wrapper code, etc. While these codes were leveraged to the extent possible, this application was novel and atypical. In the event that project personnel, in communication with developers of the codes in question, determine that it is easier to write novel code rather than adapt existing, this was done. In these cases, the novel code likely represents a low-fidelity approximation.

A risk not fully considered at the outset of the project was that the modeling of attenuator dynamics in existing software (particularly WecOptTool) was more difficult than expected. Traditional modeling and system identifications techniques proved insufficient. While it required beginning the project to fully understand this risk, having an additional contingency included here could have prevented some inefficiencies. In retrospect, in the event of insufficient techniques in WecOptTool, the team would quickly pivot to a simple heave-only (using relative heave to estimate pitch) model of the attenuator or a simple WEC-Sim model while narrowing the scope of analysis as necessary.

Signal Description Boundary element suitable meshes for all WEC configurations WEC dimensions considered Optimal parameter sets (Table 2) identified by wecOptTool WecOptTool optima for given sea states for promising configurations WecOptTool model Code and data needed for users to run the developed WecOptTool model WEC-Sim model(s) Code and data needed for users to run the developed WEC-Sim model(s) Time-domain data Output structure from WEC-Sim models, containing all timedomain simulation data for sea-states and device configurations of interest Link https://mhkdr.openei.org/submissions/644

Table 3: Data to be submitted to MHKDR.

6.3 Data Management, Processing, and Analysis

6.3.1 Data Management

Codes, models, and results were uploaded to a private GitHub repository accessible only to Marson and Sandia personnel. This facilitated collaboration and streamlined with the WecOptTool workflow: GitHub is the most desirable installation pathway for this software. Locally, Sandia personnel stored Marson data on encrypted hard-drives for project duration.

Table 3 shows a summary of the data submitted to MHK-DR:

The WEC design, models, data, and all other relevant work are intended by project partners to be open-source: no work undertaken in this project is considered sensitive or inappropriate to release.

6.3.2 Data analysis & Processing

Optimization was performed in wecOptTool [5]. WEC hydrodynamics were calculated from Capytaine and its additional hydrostatics module [6], as described in the above section. Because explicit cost (in \$) was beyond scope, several optimization cost functions intended to act as reasonable cost (in \$) proxies were explored in wecOptTool after the trends in electrical power capture, constraint activity, and structural loads were examined in batch runs with selection of fixed geometries. First, an electrical power capture normalized by the number of generators $C_1 = P_{elec}/k$ was considered but not used because all cases had the same number of generators. Next, electrical power capture normalized by float volume $C_2 = P_{elec}/(\sum_{i=1}^k V_i)$, where V_i is the volume of the ith float. A combination of this cost function was explored, as

$$C_{1,2=c_1C_1+c_2C_2} \tag{3}$$

where c_1 and c_2 are weighting constants, but only C_2 was used in this project. The appropriate value of these constants depends on the actual component cost (in \$), and precise determination is beyond present scope, but trends in suggested optima resulting from variation of these constants yielded useful understanding. More cost functions considering additional parameters were explored, particularly if structural loads are high, or constraints on PTO applied forces were frequently active as both might be expected to drive device cost (in \$).

Table 4: Wavelength (m) range from min/max wave height and periods

| | T = | T = 2, | T = | T = 2, |
|----------------|-------|---------|---------|--|
| | 17, | h = 0.5 | 17, | $ \begin{array}{ccc} T &=& 2, \\ h &=& 5 \end{array} $ |
| | h=5 | | h = 0.5 | |
| Deep water | 451.2 | 6.2 | 451.2 | 6.2* |
| Shallow water | 14.0 | 119.1 | 14.0* | |
| (d = 5m) 119.1 | | | | |

Table 5: Wavelength (m) from targeted wave height and periods

| | T = 11, | T = 7, | T = 11, | T = 7, |
|---------------|---------|--------|---------|--------|
| | h=3 | h = 1 | h = 1 | h = 3 |
| Deep water | 188.9 | 76.5 | 188.9 | 76.5 |
| Shallow water | 77.0 | 49.0 | 77.0 | 49.0 |
| (d = 5m) | | | | |

Time-domain modeling was performed in WEC-Sim [7] to the component level. All displacements, loads, and power (where relevant) generated by each component was logged by WEC-Sim and compared statistically to WecOptTool outputs: particularly structural loads on each buoy, the PTO, generated electrical power, and the extent to which any kinematic or dynamic constraints were active was compared. Substantial differences could indicate that the non-linearities and higher fidelity of the WEC-Sim model were significant to these performance metrics compared to the simpler dynamic models in WecOptTool, and that the accuracy of the WecOptTool model may be iteratively improved by performing system identification (see, for example [4]) on WEC-Sim output data and updating WecOptTool with the identified models.

7 Results

7.1 GEOMETRY PARAMETER RANGES

Basic wave theory and some intuition is used to bound the length parameters that were used to parameterize float geometries. Using the dispersion relation for deep water waves

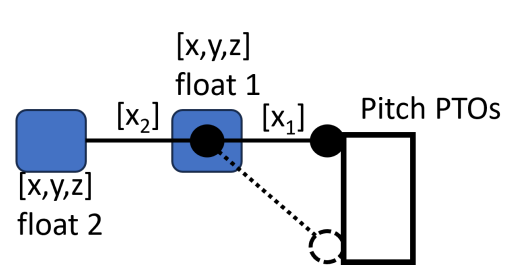
$$\lambda = \frac{g}{2\pi} T^2 \tag{4}$$

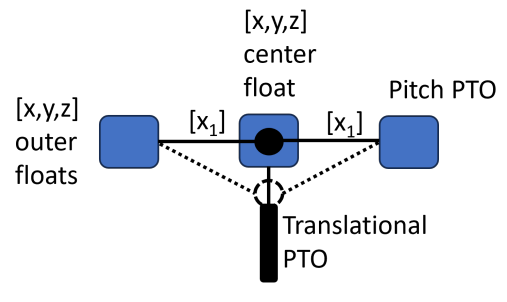
and shallow water waves

$$\lambda = T\sqrt{gd} \tag{5}$$

the relationship between wave length λ (m) and the sea-state parameters period T (s) and water depth d (m) for a given gravitational acceleration constant 9.81 (m/s²). For the minimum and maximum h and T in wave range shown in Table 1, this corresponds to the wave lengths in Table 4, where unstable breaking waves are indicated with an asterisk.

The suggested wavelengths of interest here range from 6.2 m to 451 m, two orders of magnitude. Considering the smaller range of targeted sea-states, the suggested wavelengths of interest range from 76.5 to 189 m. Because the predominant mode of energy capture will be the relative pitch displacement of adjacent bodies or adjacent groups of bodies, body/group length equal to one-half the wave length in the direction of propagation is likely to maximize





- (a) Fixed end WEC configuration diagram.
- (b) Floating WEC configuration diagram

Figure 6: Fixed end vs. floating WEC setup. The dashed lines and circles represent the drop PTO configuration which may better capture surge motion.

pitch excitation, or 38.3 to 94.5 m. Visualizing the system as in the right hand side of Figure 3, the reasonable length of each span between adjacent generators $r_{g,i} - r_{g,i-1}$ is an approximate function of the number of floats to be considered. a priori, an upper limit of N = 6 is selected, recognizing that BEM computational complexity increases by $6N^2$. Thus, maximum device extents ranging from 15 m (approximately 94.5/6) to 95 m are selected.

Two different configurations were considered on top of the geometric, PTO, and control parameters to be explored. The first is (left side of Figure 6) characterized by a fixed end on the leeward side and rotational PTOs connected to a series of floats. This means the rightmost float acts against a stationary PTO and a second PTO rotates according to the relative position between the two floats. It is expected that the fixed end configuration may favor relatively short distances between floats to reduce the amount of PTO torque needed while still achieving large PTO rotations relative to the fixed end. The second configuration (right side of Figure 6) is a floating WEC with a translational PTO connecting a mooring cable to the central float and rotational PTOs connecting to floats on either side. Because the PTOs will be based on relative motion between floats, it is expected that the floating configuration favor relatively long distances between float closer to the wavelengths in Table 5. For both configurations, a flat PTO and a drop PTO (in which the PTOs are placed below the floats to capture surge and heave energy) were tested.

7.2 BOUNDARY ELEMENT METHOD

The calculation of multiple hydrodynamic bodies in the broad parameter space is computationally demanding. The hydrodynamic coupling between nearby bodies, however, may not always be significant. To reduce computational complexity, the hydrodynamic bodies were solved individually and then later combined. This implies that once solved individually, a body can be freely moved in horizontal space without recalculating boundary element method for each position by phase-shifting excitation coefficients [7]. This neglects hydrodynamic coupling between floats during the initial investigation: however, top-performing contenders were validated in WEC-Sim using BEM runs including hydrodynamic coupling.

It is possible that this method misses advantageous hydrodynamic coupling that would have otherwise suggested alternative morphologies as top performers. This shortcoming is acknowledged, however to address this wholly would have greatly exploded the scope to an array optimization problem in addition to the float geometry, PTO, and controller optimization that is intractable in the current investigation.

7.3 LIMITATIONS OF WECOPTTOOL FOR ATTENUATOR WECS

The original planned scope of work was to perform the hydrodynamic parameter sweep in WecOptTool. However, this was not attainable due to some restrictions to the dynamic model setup in WecOptTool. The coupling between the WEC response and the resultant PTO force on the WEC could not be directly defined with WecOptTool's current setup without simplifying the model beyond physical relevance. WecOptTool has been used for a number of point absorber type WECs and is a powerful tool for optimization, but it has not yet been demonstrated for an attenuator type WEC. A number of potential solutions were explored for modeling the attenuator in WecOptTool considering a simple two-body concept with one end fixed:

- To provide a simple starting point, the team started with only considering 1 degree of freedom heave motion for each body. While this solution proved tractable and efficient for WecOptTool, it did not make sense physically. Assuming only heave motion left a vital question unanswered: how do the PTOs (located between each successive float) move relative to the floats. In the physical system these would move based on the pitch of each float, but without the pitch degree of freedom resolved, the PTO locations would need to be found based on the heave of each float. Any assumption of PTO location based on heave is significantly limiting and this starting point was not found to be a sufficiently accurate model.
- Notably only pitch motion is not a reasonable assumption because the PTO location would either need to be assumed to be constant (physically not true) or the dominating heave hydrodynamics would be missing.
- Next, a multi-degree of freedom (heave and pitch) attenuator model was explored. With multiple degrees of freedom, the PTO locations would be defined according to the pitch of the individual floats. WecOptTool requires a kinematic matrix to define the conversion between the WEC degrees of freedom and PTO degrees of freedom. Starting with a simple one body attenuator pitching about a fixed PTO, the kinematics matrix, K, can be defined by relating the WEC degrees of freedom \dot{x} to the PTO degrees of freedom \dot{p} .

$$\dot{p} = K\dot{x} = \begin{bmatrix} 0 & 1 \end{bmatrix} \begin{bmatrix} \dot{z}_1 \\ \dot{\theta}_1 \end{bmatrix} \tag{6}$$

However, WecOptTool also uses the inverse of the kinematics matrix to define the forces from the PTO onto the WEC. Based on the above K, the force from the PTO would only act on the pitch degree of freedom:

$$F_{WEC} \neq \begin{bmatrix} 0 \\ 1 \end{bmatrix} F_{PTO} \tag{7}$$

Thus, it is not possible to solve the full dynamics of the attenuator WEC using only a traditional BEM setup and the existing kinematics matrix in WecOptTool.

• Despite the kinematics matrix not being a valid option on its own, it may still be possible in conjunction with another approach. WecOptTool allows for constraints on body motion to be applied, meaning the heave can be constrained according to the PTO's pitch. However, to maintain the constraint, WecOptTool requires a separate

optimization variable in the respective degree of freedom to enforce the constraint. To test this implementation, the following constraint was placed on the heave degree of freedom and an optimization variable added to heave.

$$z = -d\theta_{PTO} \tag{8}$$

Unfortunately, the additional optimization variable (defined at every timestep) doubled the number of optimization points and led to convergence issues that were not able to be resolved. While this approach may offer a solution in theory, optimization limitations prevented it's feasibility.

• An approach that was not able to be fully explored is utilizing Capytaine to define the pitch degree of freedom for each float about the previous float as a generalized mode. Then, the BEM coefficients would be resolved for the relative pitch between two successive floats. The mass and hydrostatics would then need to be converted accordingly. This was outside the scope and budget of this project but likely offers a solution for future WecOptTool modeling of attenuators.

While the team does believe there is a solution for modeling the system strictly in WecOpt-Tool, additional work in this space was outside the scope and budget of this project.

7.4 GENERALIZED BODY MODE APPROACH

Another potential method of modelling an attenuator consisting of multiple floats with relative pitch motion is using generalized body modes (GBM). A generalized body mode is a mode of body motion outside of the normal 6 degrees of freedom and can be defined when solving the boundary element method. By using GBM, the problem of interacting hydrodynamic bodies (Section 7.2) can potentially be avoided because the system is instead characterized by one segmented float. Two possible approaches for using GBM to model the attenuator WEC have been explored:

- Often, GBM is used to characterize flexible bodies and requires defining the mode shapes. While modeling the attenuator WEC as one long, flexible float is an option, it presents a number of design challenges. For example, the material properties and damping of each mode shape needs to be defined, potentially adding more design variables to an already complex problem. Further, while the results can provide the flexible body's response, translating the flexible response to the performance of the attenuator WEC requires additional assumptions. While GBM with flexible modes may be an option, it was not pursued further due to the additional challenges and unclear definitions.
- GBM can also be used to define a hinge in which one portion of the float is rotating relative to another portion. This approach provides a more tractable translation to the attenuator WEC where one hinge of the GBM float is directly comparable to a PTO hinge in the attenuator. The problem does require manual calculation of hydrostatics and conversion of the force to the hinge location but the solution is straightforward. The system would be solved at the PTO hinge and the PTO response would be calculated as a result which would translate easily to float responses. This can provide an alternative for modeling the attenuator WEC in the future. It may also be an option for modeling the WEC directly in WecOptTool without needing to relate multiple degrees of freedom to each PTO.

Notably, the GBM approximation was intended for a single, continuous, flexible float. However, early optimization results indicate that individual floats, separated by some significant distance, is more likely to be a cost-effective approach. In theory, a generalized body mode can be introduced between multiple floats captured in a single mesh file. At project start, it was unclear whether this approach is valid computationally: in retrospect, it is a valid approach and should be considered for optimization of attenuator-type devices in the future.

7.5 IMPEDANCE AND EXCITATION IDENTIFICATION

In lieu of kinematic description and impedance modeling in WecOptTool, a reduced set of models were run in batches in WEC-Sim following the method of [4]. Because this approach takes substantially more time than WecOptTool, the space was reduced to two-body systems with one end fixed, and symmetric three-body free-floating systems (Figure 6). Further, the PTOs were made coincident with the body adjacent to the fixture (in the first case) and coincident with the central float (in the second case). The parameter space studied can be found in Table 9 in the Appendix. With this simplification of geometry, the azimuthal sweep angle becomes irrelevant: a rectangular float will always deliver more excitation to the bodycoincident PTO per float volume, because it would be parallel to the wave crest. It was intended that these identified impedance and excitation models would be used subsequently in wecOptTool for optimization, but this imposed some additional challenges: a negative real part of the impedance at any frequency over the investigated range appears to an optimizer as a negative damping, and a non-physical opportunity to generate infinite energy. At this time, the strong coupling between the device degrees of freedom and/or the kinematic linkage implied by attenuator type devices result in PTO velocities that are highly correlated (even when their forcing signals are, by design, uncorrelated) is believed to somewhat confound the system identification procedure. To circumvent this, an two alternative approaches were applied. First, for pitching-type PTOs, all but one of the PTOs was locked, and the on-diagonal impedance elements were identified sequentially. The off-diagonal impedance elements were identified through simultaneous excitation of all PTOs. Secondly, for the heave-type PTO of the three-float floating system, the impedance can be estimated analytically from the BEM coefficients in heave as the linear superposition of each body impedance as

$$Z_{33} = Z_{u,33} + Z_{c,33} + Z_{d,33} \tag{9}$$

where $Z_{u,33}$ is the heave impedance of the upwave float, the subscripts c and d indicate the center and downwave float. Similarly, calculating excitation in a manner consistent with [4], in which the excitation model is a derived quantity dependent on a previously identified impedance was challenging owing to the negative real parts. Instead, a more traditional approach of locking all power take-offs and exciting the locked device with pink-spectrum waves was adopted. The excitation function then was calculate in the frequency domain as

$$f_{exc} = F_{exc}/\eta(\omega) \tag{10}$$

where $\eta(\omega)$ is the wave height spectrum and F_{exc} is the excitation force as measured at the locked constraint. This estimation procedure is effectively a distinct linearization of the excitation coefficients that is identical to BEM estimates, just in a different coordinate system.

This approach resulted in useful impedance estimates that were sufficient to proceed with WecOptTool optimization, however the difficulty noted with the identification procedure suggested in [4] for closely coupled systems or systems in which PTOs are arranged in a

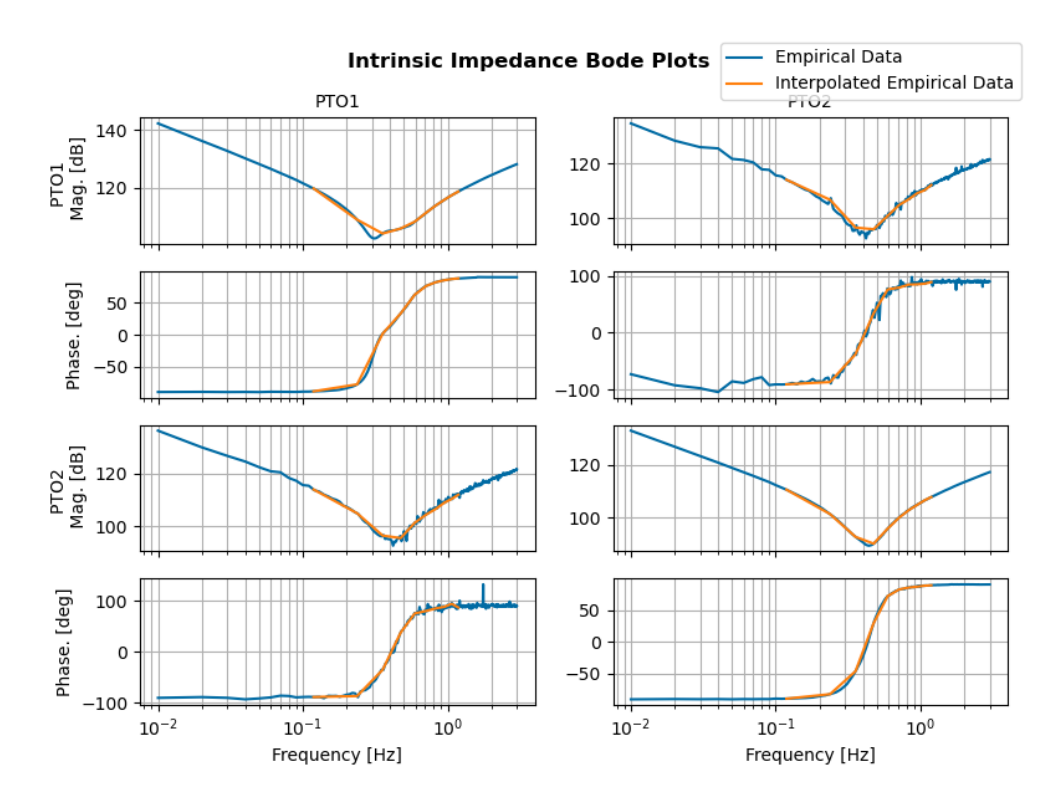


Figure 7: Example of impedance data from system identification and the interpolated result used for WecOptTool.

kinematic chain warrants further investigation. Similar challenges were observed in [8], but the coupling was insufficient to confound the methodology.

7.6 WecOptTool Impedance-Based Approach

Using the impedance and excitation models identified in Section 7.5, WecOptTool models can be developed for each configuration. For a two body system, the impedance model consists of a 2x2 matrix for each frequency with the diagonal terms representing the impedance of the system relative to each PTO and the off-diagonal terms representing the interactions (and coupling forces) between the PTOs. Figure 7 plots the impedance matrix with the top left two plots being for PTO 1 (leeward side) and the bottom right two plots for PTO 2. Since the coupling terms are handled in the impedance matrix, the WecOptTool kinematics are defined simply as a one-to-one conversion (i.e., the first impedance DOF corresponds directly to the first PTO DOF). WecOptTool requires defining a frequency array at which the wave and WEC dynamics are simulated. The frequency array is selected to include the input wave conditions and resulting response. The impedance and excitation are then interpolated along the frequency array, as detailed in Figure 7 and 8. Note that the interpolation may not capture all features of the impedance but is uniquely sufficient for each wave condition analyzed. Oscillations in excitation phase as frequency increases are consistent with similar floating bodies. For frequencies above the range of identification, the excitation is interpolated to 0 (following clear trend in plots).

A wide range of variables were investigated during the system identification process. Based on the range of configurations tested, the following variables have been identified for comparisons within the WecOptTool analysis:

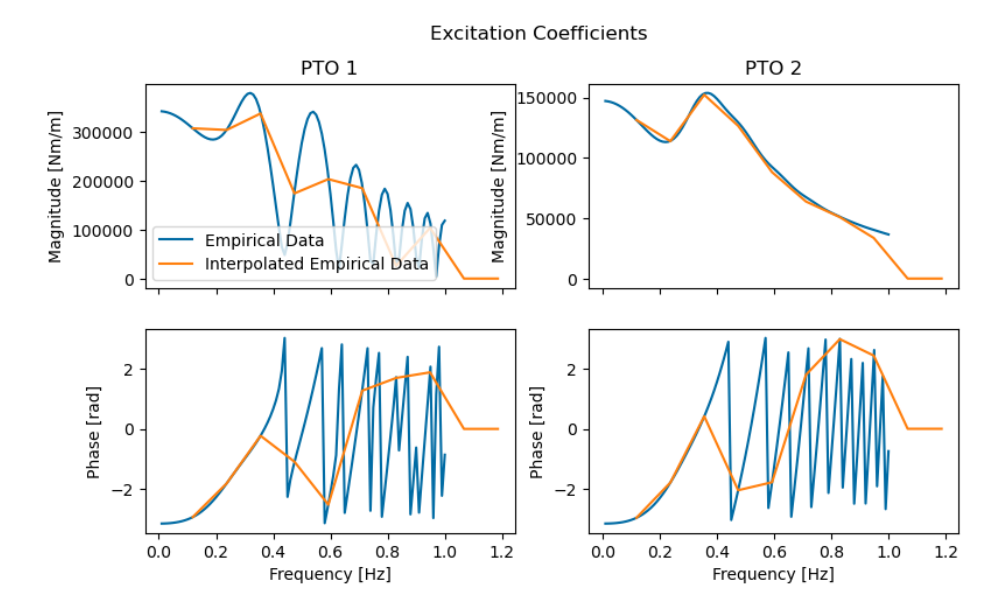


Figure 8: Example of excitation data from system identification and the interpolated result used for WecOptTool.

Table 6: Siemens COTS generator parameters

| Parameter | Value | Units |
|--------------------|--------|----------|
| Torque Constant | 13.1 | Nm/A |
| Winding Resistance | 0.0125 | Ω |
| Winding Inductance | 0.65 | Н |

- Drop PTO versus flat PTO
- Distance between floats
- XYZ dimensions

There are also a number of PTO parameters to be investigated to better understand the system from a co-design perspective. By considering PTO design at this stage through co-design, design decisions can be made with a greater knowledge of impacts to system performance and further design implications. First, a generator was selected (Table 6) based on Siemens commercial-off-the-shelf (COTS) options for a system of this size. While this does restrict the design space (and may exclude some well-performing designs), it also tractably constrains the problem to realistic bounds.

The PTOs are each defined as an impedance model as in [9]. Aside from the generator, other PTO parameters considered for analysis here are:

- Gear ratio (default: 10)
- Drivetrain inertia (default: 0 kg m²)
- Drivetrain stiffness (default: 0 Nm/rad)
- K_p , K_i control gains

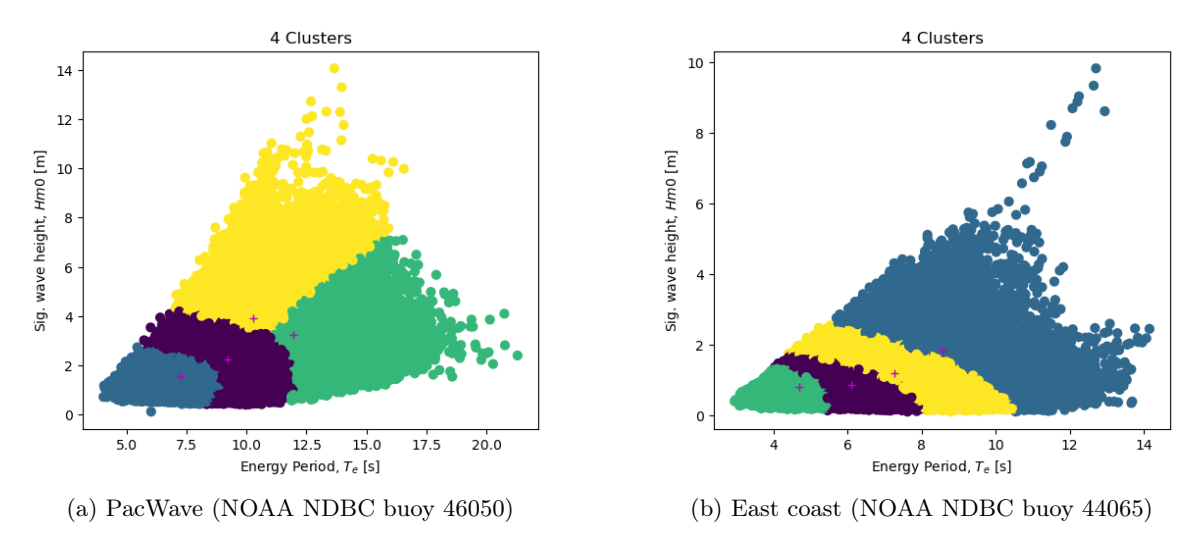


Figure 9: Wave conditions clusters identified for two different locations in the US. The clusters are represented by different colors and the red x's are the wave conditions used to represent each cluster.

The gear ratio, drivetrain inertia, and drivetrain stiffness were each examined through a parameter sweep for some of the best performing dimensional configurations. However, the K_p and K_i control gains are the main optimizations variables in this study. For each result presented here, the K_p and K_i gains have been optimized to achieve maximum average power within the constraints. For constraining the system, a maximum rotation angle of 45 degrees was considered to avoid unrealistically large motions and remain within the ranges of linear theory.

7.6.1 Wave conditions

Two different locations are considered for optimizing and examining the WEC's performance. First, PacWave is a marine energy testing site that provides reference for a large wave environment. The PacWave wave conditions were derived from NOAA NDBC buoy 46050 and divided into 4 clusters using k-means clustering (right side of Figure 9). The other location considered is in the Atlantic Ocean off the coast of New York City (NOAA NDBC buoy 44065). This location will be referred to as the east coast location and was chosen for its smaller wave environment (where this device may be more successful) but proximity to population centers. The left side of Figure 9 shows the 4 clusters for the east coast location.

7.6.2 Drop PTO vs. flat PTO

For each dimensional configuration modeled in the system identification, there were two cases: one with the PTOs vertically in line with the floats ("flat") and one with "drop" PTOs where linkage between the first float and the fixture is 45^o below the waterline. The drop PTO is explored so that a component of both surge and heave excitation will act on the un-displaced PTO, which may change optimal results. To compare the drop versus flat PTO, all of the configurations were run in both the conditions from PacWave and from the east coast. After running the optimization for these cases, the total average power was compared for the different wave conditions between the two PTO positions (negative power is power harvested by the WEC). Overall, the results are not entirely conclusive. For some configurations (e.g.,

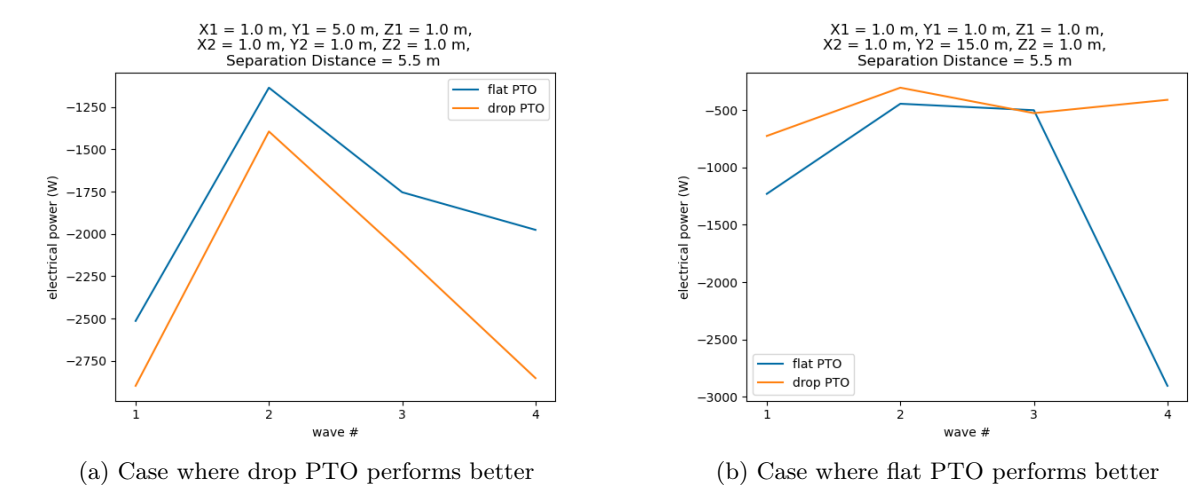


Figure 10: Drop vs. flat PTO for two different configurations in the 4 east coast clusters (Figure 9).

with a large float 1 and small float 2 with 5.5 m between bodies), the drop PTO performs better, but for others (e.g., with a small float 1 and a very large float 2 with 5.5 m between bodies), the flat PTO performs better as detailed in Figure 10 (for east coast waves).

While the overall results are not entirely conclusive between the drop and flat PTO, there are still a number of insights that can be gained. Looking at the impedance plots for the first case (large float 1 and small float 2) (Figure 25 in the Appendix), it is clear that PTO 1 impedance has a relatively shallow trough (larger minimum value). This means excitation force is translated into lower velocities, but the excitation forces for PTO 1 are also larger (Figure 26 in the Appendix) which may compensate for the larger impedance. The shallower trough for the drop PTO is also wider which means that the bandwidth is wider and the system responds more to a range of wave periods. This likely contributes to the increases in total average power.

While the second case (small float 1 and very large float 2) does provide an example of the flat PTO performing better than the drop PTO, it only performs better for three out of the four wave conditions. This is consistent with other cases that showed the flat PTO performing better. Because the drop PTO seems to lead to a wider bandwidth, it leads to more consistent results than the flat PTO. When considering all of the configurations, the drop PTO more consistently leads to greater average power. To efficiently narrow the search field, the flat PTO is excluded from some of the following analyses.

7.6.3 Distance between floats

For each float dimension combination, two cases were run: one with a shorter distance between the floats and one with a longer distance between floats. While the exact distances were varied relative to the float dimensions, the overall trends remained consistent. In both PacWave and east coast wave conditions, the cases with shorter distances generally perform better.

To understand why the shorter distance cases perform better, it is useful to compare two cases with equal float dimensions but one with a longer distance between floats and one with a shorter distance. The "shorter" distance is a case in which float 1 is located at x=-1 m and float 2 is located at x=-2.5 m. The "longer" distance is a case with float 1 at x=-5 m and float 2 at x=-10.5 m. From Figure 11, it is clear that the shorter case leads to

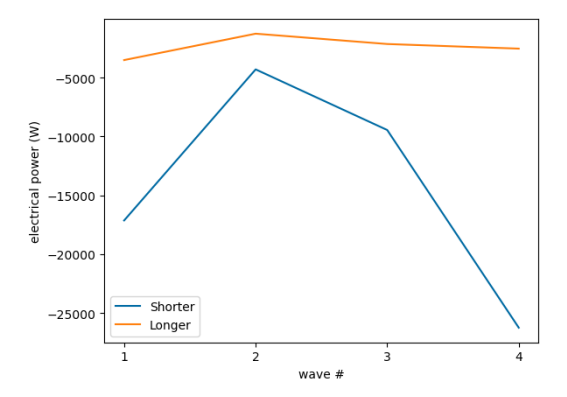


Figure 11: Total electrical power for shorter vs. longer distances in the 4 east coast clusters (Figure 9).

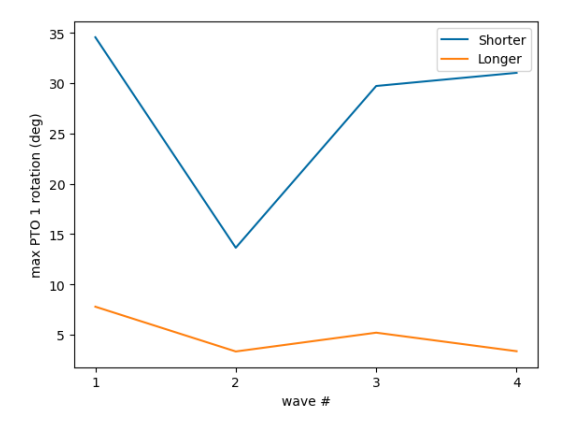


Figure 12: PTO 1 maximum rotation for shorter vs. longer distances in the 4 east coast clusters (Figure 9).

significantly more power.

Examining the PTO response Figure 12, the maximum rotation is much smaller in all wave conditions for the slightly longer PTO. While this is reasonable for the case with a stationary PTO on one end (a longer distance means heave of the float translates into less rotation), it means that a larger PTO torque would be required to achieve the same mechanical power. However, the PTO torque (Figure 13) is actually lower for the longer distance. This is because with a lower PTO rotation, the velocity is small for the selected generator and the power is limited by the generator's resistive (I^2R) losses. Higher torques may achieve more mechanical power but would further reduce the velocity, leading to less electrical power.

It is important to note that the selected gear ratio (10) can significantly impact these results. A larger gear ratio increases the velocity at the generator and can reduce losses (especially for the longer distance). However, the larger gear ratio would increase frictional losses not taken into account here. The impacts of gear ratio are explored further in Section 7.6.5.

In terms of the impedance and excitation (Figure 29 and 30 in the Appendix), the impedance from the longer case is much larger in magnitude, meaning more force is needed to achieve the same velocity. While the excitation force is also larger for the longer case, it is not significant enough to make up for the larger impedance. This makes sense as heave motion of the float with a short lever arm has a greater contribution to the PTO rotation when fixed on one end than for a long lever arm. Thus, in combination with the generator

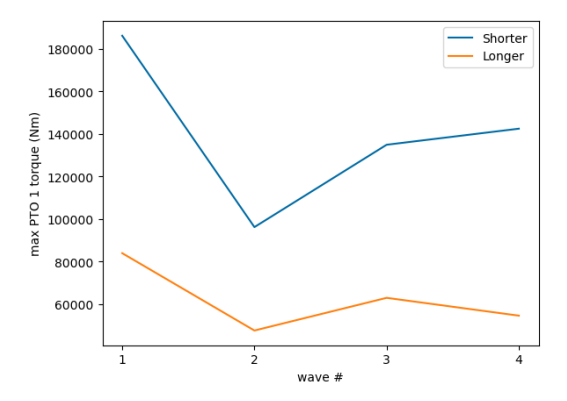


Figure 13: PTO 1 maximum torque for shorter vs. longer distances in the 4 east coast clusters (Figure 9).

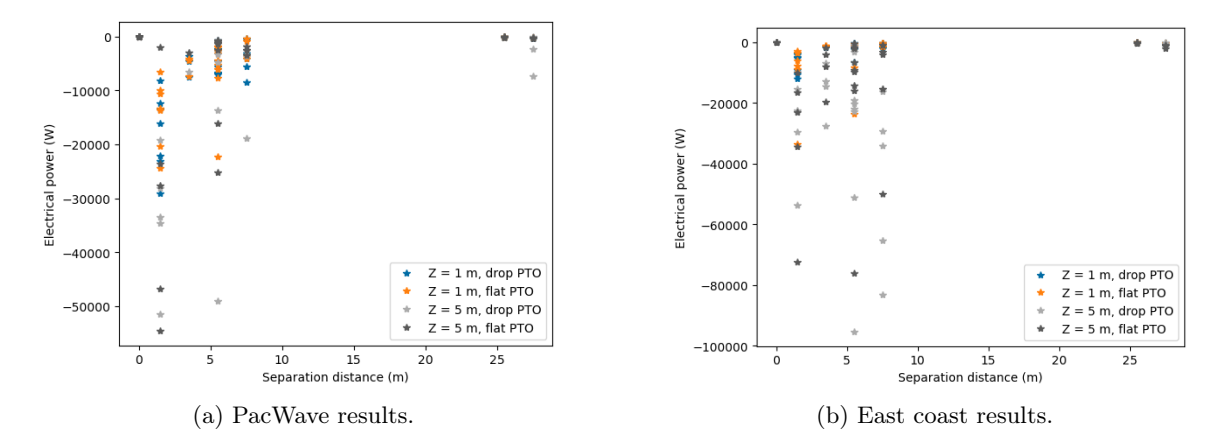


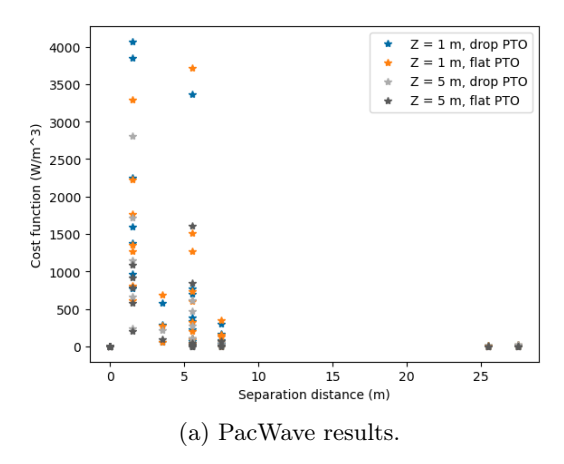
Figure 14: Electrical power versus separation distances for different configurations at both locations considered. Other changing parameters are the x and y dimensions of the each float.

losses, the smaller impedance magnitude allows the shorter case to achieve much higher velocities and a higher average electrical power. Alternative PTO selections may have some impact here: namely, a hydraulic system may be well-suited for the high-torque low velocity applications, and very large gear ratios, provided they do not introduce large friction, may also change the balance of the quantities concerned, but the fundamental trade-off between increased impedance and increased excitation will remain relevant.

7.6.4 XYZ dimensions and identification of top performers

The drop versus flat PTOs and the float distances can first be compared directly by the average electrical power in Figure 14. On the other hand, the float dimensions cannot easily be compared by electrical power, because a much larger float can achieve larger electrical power but costs significantly more. In order to more holistically compare the performance across different dimensions, the cost function from Eq. (3) can be used. Because all of the cases here have 2 PTOs, only the second term of Eq. (3) will be used by dividing the average power by the total float volume.

The cost function was evaluated for all of the cases in both the PacWave and east coast conditions (Figure 15). Note that a few cases have a cost function of 0 which is filler value



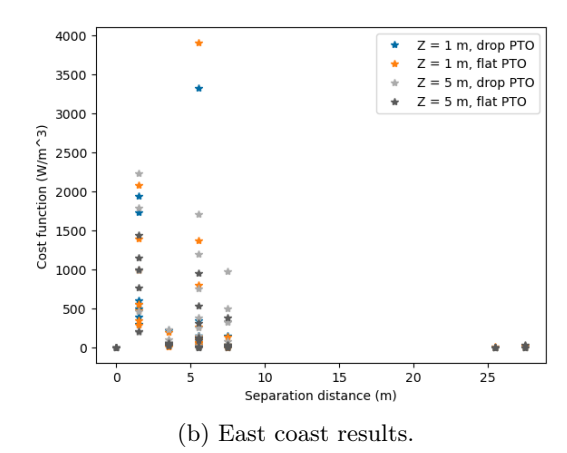


Figure 15: Cost function versus separation distances for different configurations at both locations considered.

for those where the optimization was unable to converge. Investigating the reasons for convergence issues is outside the scope of this study, but these cases mostly seem to be for larger dimensions/volume where the cost function values were smaller anyway. Further, the trends are still visible despite convergence issues. While the Z=5 m cases lead to larger electrical power, the 5x increase in volume is often not worth it as identified by the cost function. Similarly, the smaller dimensions generally performed well compared to larger dimensions. In alignment with Section 7.6.3, these are also associated with shorter distances between floats.

For the east coast wave conditions, the results were relatively similar. The smaller floats and shorter distances gain performed best for both the $Z=1~\mathrm{m}$ and $Z=5~\mathrm{m}$ cases, but the $Z=5~\mathrm{m}$ cases performed more similarly to the $Z=1~\mathrm{m}$ cases in these smaller wave conditions. Based on these results, some $Z=5~\mathrm{m}$ cases should also be considered in further studies. Notably, small floats separated by relatively small distances (1 to 5.5 m separation distance) performed best. Since these two distances both performed well, it is expected that the optimal separation distance lies in the 1 to 5.5 m range for the fixed end PTO. Since longer distances between floats will be associated with less PTO rotation, they therefore require more PTO torque and are likely limited by the PTO and generator parameters to be explored further in Section 7.6.5.

Combining the assessment in PacWave and east coast wave conditions, a subset of the WecOptTool investigated morphologies can be identified as top performing, contrasting, or otherwise interesting case studies for evaluation in WEC-Sim. These case studies are specified in Table 7.

The WecOptTool results discussed here provide valuable information about the nature of the fixed end WEC systems, but comparisons to WEC-Sim yielded less than justifiable matches between models. This is believed to be due to some issues with the impedance and excitation models themselves (to be discussed further in 7.9. Thus, while some insights were gained in this section, discussion of the WEC-Sim model below provides a more accurate profile of the system.

7.6.5 PTO parameters

Using the best performing cases from the WecOptTool optimizations, the PTO parameters can be investigated in more detail for the down-selected buoy geometries.

Table 7: Best-performing cases (dimensions in m) based on WecOptTool optimization in PacWave and east coast wave conditions. Note that each count has two cases: 1 m and 5 m Z-dimension. Refer to Table 9 for a summary of all cases tested.

| - Ct | | F | loat 1 | | | F | loat 2 | |
|-------|---|---|--------------|-------|---|---|--------------|-------|
| Count | X | Y | \mathbf{Z} | X loc | X | Y | \mathbf{Z} | X loc |
| 1 | 1 | 1 | 1 | -1 | 1 | 1 | 1 | -2.5 |
| 2 | 1 | 1 | 1 | -5 | 1 | 1 | 1 | -10.5 |
| 5 | 1 | 1 | 1 | -1 | 1 | 5 | 1 | -2.5 |
| 1 | 1 | 1 | 5 | -1 | 1 | 1 | 5 | -2.5 |
| 5 | 1 | 1 | 5 | -5 | 1 | 5 | 5 | -10.5 |

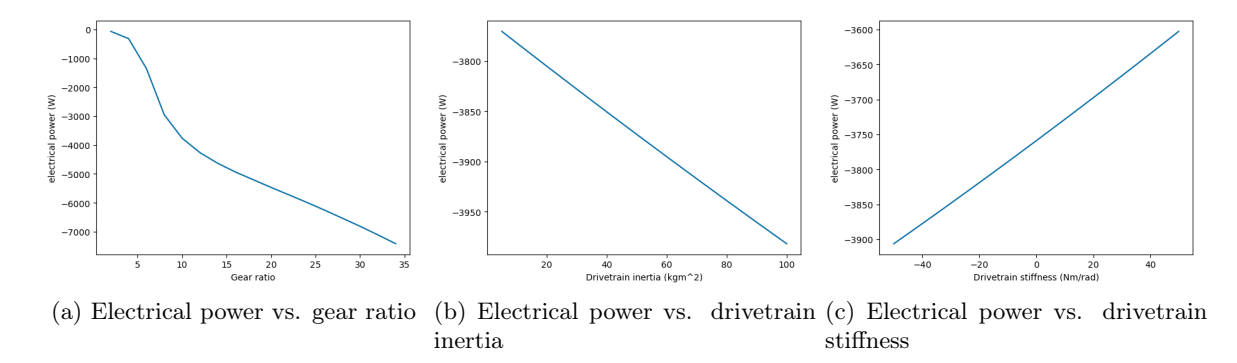


Figure 16: Electrical power versus PTO parameter sweeps for count 2 in the most common wave from the east coast clusters.

First, the three PTO parameters of interest were optimized for one of the best performing cases with small floats and a longer separation distance (count 2 Table 7) in east wave conditions. Only the most common wave of the 4 clusters was used for efficiency here. Figure 16 shows the relationships between each of the PTO variables and the average electrical power. Electrical power increases are achieved for increasing gear ratio, increasing drivetrain inertia, and decreasing drivetrain stiffness. In reality, these trends would come with tradeoffs such as increases in friction (larger gear ratio) and higher costs (negative stiffness), and it is vital to consider the tradeoffs when designing/selecting these components.

We can also consider the change in PTO parameter trends across the other variables. The drivetrain inertia and stiffness trends remain relatively consistent across different configurations but the trends relative to gear ratio change. For example, Figure 17 shows the trend in electrical power as a function of the gear ratio for the longer and shorter float distances. The trends for the shorter gear ratio were less consistent due to convergence challenges, but insights can still be gained. For the lowest values of gear ratio, the shorter distance leads to larger power, but the longer distance significantly outperforms as gear ratio increases. The larger gear ratio enables the generator to experience higher velocities and provide more torque back onto the system. While this is valuable for both cases, its impacts to the longer PTO are greater because it was limited by torque (as discussed in Section 7.6.3). Increasing the gear ratio does help for this longer distance case (which is still among the shorter cases overall), but the gear ratio can only be increased so much before efficiency and friction become larger concerns. Considering the costs (physical and economical) of gear ratio and float distances would likely lead to an optimal design that balances increasing distance between floats (to

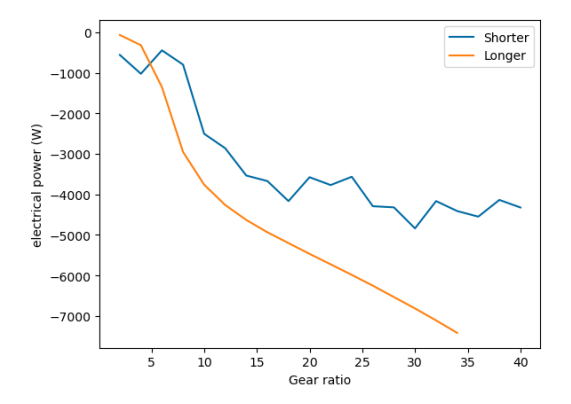


Figure 17: Electrical power vs. gear ratio for two different float separation distances in the most common wave from the east coast clusters.

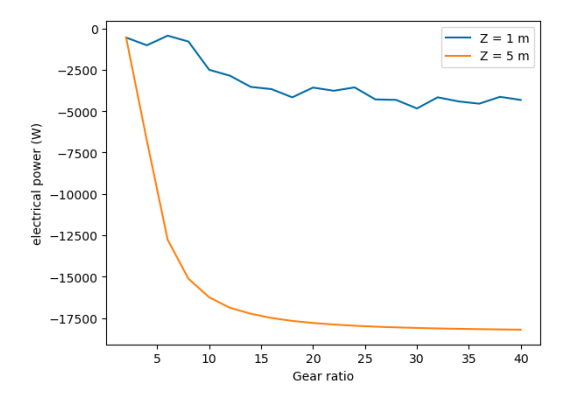


Figure 18: Electrical power vs. gear ratio for two different Z dimensions in the most common wave from the east coast clusters.

increase relative motion) and increasing gear ratio (to allow for more generator torque).

Another factor that can impact the trend of electrical power with respect to gear ratio is the Z dimension. For a smaller WEC ($Z=1~\mathrm{m}$), the electrical power is significantly smaller, but the overall trend remains relatively consistent (Figure 18). For both Z dimensions, the electrical power plateaus for gear ratios about around 12. This is because the PTO rotation constraints are met (45 degrees) and any larger torques would exceed the efficient range of the generator.

While the PTO torque is limited by the generator I^2R losses, the PTO velocity (at the generator) is not limited without any friction. Hence, it tracks that a larger gear ratio always performs better in Figure 17 and Figure 18. However, with drivetrain damping included (B), the problem now becomes a balance between the hydrodynamic radiation damping, generator I^2R losses, the friction losses in the drivetrain, and the gear ratio, which each contribute to an optimal design point to maximize the electrical power (Figure 19). The motor constant K_t (N-m/A), here fixed, will also affect this relationship. The selected drivetrain and generator will thus dictate the optimal gear ratio.

7.6.6 Floating cases

This section details the results from analysis of the floating configuration shown in Figure 6 b in WecOptTool. The central float is connected to a translational PTO and the outer floats

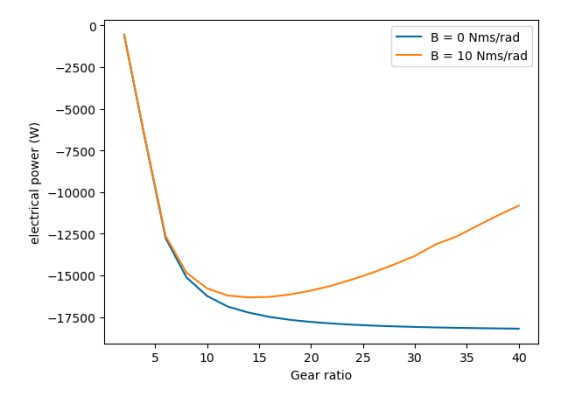


Figure 19: Electrical power vs. gear ratio for two different drivetrain damping values in the most common wave from the east coast clusters.

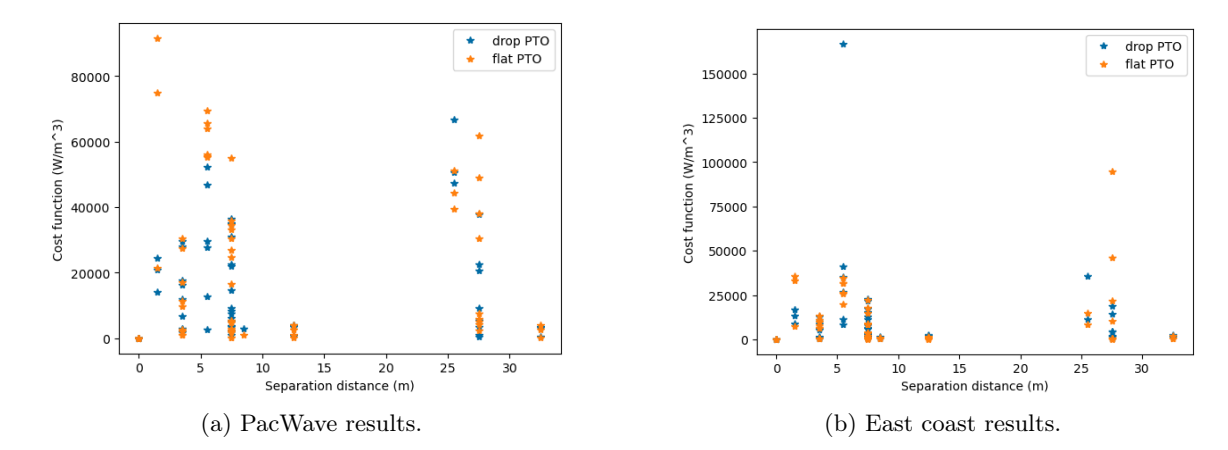


Figure 20: Cost function versus separation distance for different configurations for the floating case at both locations considered.

are connected to the central float via rotational PTOs.

The results in terms of the evaluated objective function in both PacWave and the east coast wave conditions are shown in Figure 20. From these plots, there are a few takeaways. First, the shorter separation distances (similar to fixed-end cases) are generally performing better which primarily have smaller float sizes. But, there are some larger separation distances cases which also perform well. For example, a case which has a large center float and medium sized outer floats spaced 27.5 m apart performs well in both PacWave and east coast wave conditions. The flat PTOs actually seem to perform better in the larger PacWave conditions while the results are relatively similar in east coast conditions (aside from an outlier). It is believed that the larger wave conditions produce sufficient heave excitation to meet the limits of the PTOs without the impacts from surge that are present in the drop PTOs but this warrants further investigation. When comparing to the fixed end cases, the floating cases have much higher objective function values across the board suggesting that the floating WEC can perform better than the fixed end WEC relative to the cost.

When considering the power in each PTO (Figure 21), it becomes clear why the floating cases perform better than the fixed end cases. The heave PTO is dominating the amount of power being generated compared to the rotational PTO for all cases considered. In some cases the optimal controller inputs power from the rotational PTOs to maximize power in

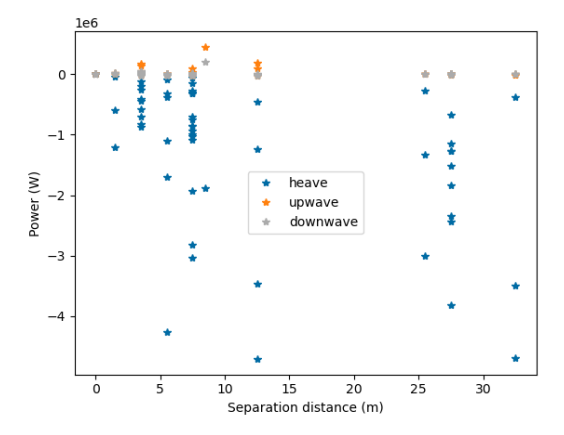


Figure 21: Power for each PTO (heave, upwave, downwave) versus separation distance (flat PTO in PacWave conditions).

Table 8: Dimensions (m) for selected floating WEC design case

| Count | | Center f | loat | | Outer fl | oats | Compandian distance |
|-------|---|----------|--------------|---|----------|--------------|---------------------|
| | X | Y | \mathbf{Z} | X | Y | \mathbf{Z} | Separation distance |
| 20 | 5 | 5 | 1 | 5 | 1 | 1 | 27.5 |

the heave PTO.

The WecOptTool results discussed here provide valuable information about the nature of the floating WEC systems, but the results do not match well when comparing to WEC-Sim. This is believed to be due to some issues with the impedance and excitation models themselves (to be discussed further in Section 7.9. Thus, while some insights were gained in this section, discussion of the WEC-Sim model below provides a more accurate profile of the system.

7.7 TIME-DOMAIN CASE STUDIES

Initial comparisons between WecOptTool and WEC-Sim yielded less than optimal results. In many cases, the gains derived for the WecOptTool models were much larger than were feasible for the WEC-Sim models. Most consequentially, large negative Ki (negative stiffness) gains often matched or exceeded hydrostatic forces/torques causing the models to go unstable. Furthermore, when gains were reduced to reasonable limits, the power was much less than predicted by the WecOptTool models. This limitation and the corresponding lessons are discussed further in Section 7.9.

For the sake of this project and the budget limits, the focus of the time-domain case studies was shifted to consider the future of the Marson WEC. If the Marson WEC can perform better than other similar WECs than it is at least worth continuing design development. However, if the Marson WEC does not perform better than similar WECs than it is in the TSR's best interest to pursue other designs instead. In order to complete this assessment, the floating WEC setup (right side of Figure 6) will be compared to a heaving point absorber WEC of the same volume. Since the case with a large center float and medium sized outer floats spaced 27.5 m apart performed well in both PacWave and east coast wave conditions (Figure 20) and was relatively stable in WEC-Sim, it was selected for further analysis in WEC-Sim. The exact dimensions for this case are found in Table 8 and illustrated by Figure 22.

To complete the comparison, both the floating WEC setup (with a heave PTO, upwave

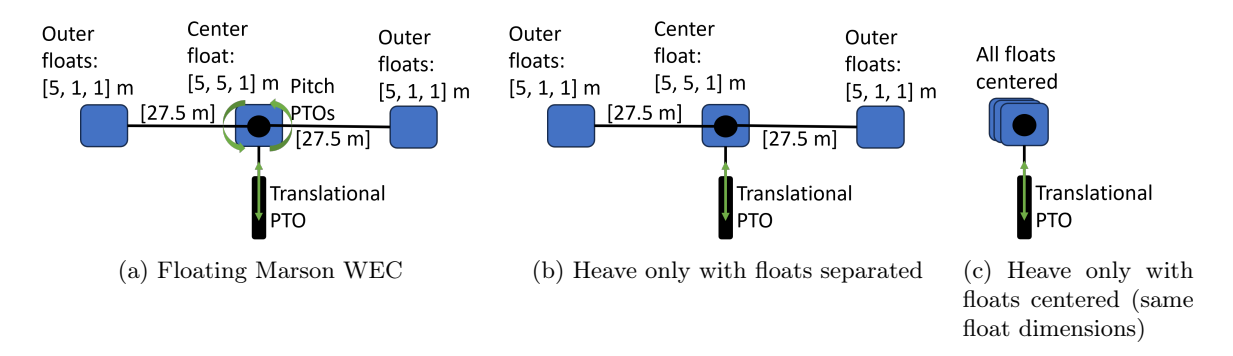


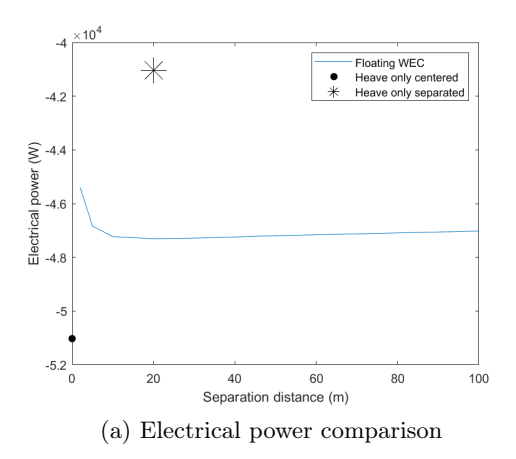
Figure 22: Floating Marson WEC for WEC-Sim analysis vs. floating heave only cases with floats centered and separated.

pitch PTO, and downwave pitch PTO) and a heave-only WEC of the same volume (with one heave PTO) were run in two wave conditions while varying the controller gains. While the controller gains were optimized in the WecOptTool analysis, these did not translate well to WEC-Sim and new ranges needed to be examined. The first wave condition was a wave representative of PacWave, and the second wave condition was a wave representative of the great lakes region (to test the system in very small/low wavelength waves).

7.7.1 PacWave Conditions

The results from PacWave conditions are shown in Figure 31 in the Appendix for the floating Marson WEC (one heave PTO, two pitch PTOs) as compared to a heave only WEC. For simplicity at this stage, the most common wave condition of the four clusters was used. For each of the plots, the electrical power is shown for a range of heave PTO proportional and integral control gains (damping and stiffness) with the same PTO parameters as from the WecOptTool model (Table 6). Rotational PTO gains were varied as well but impacts were relatively small, and only results from the best set of rotational PTO gains are shown for each plot. The first two plots in Figure 31 represent the heave-only systems. For the first plot, a heave-only WEC was simulated with equivalent mass and volume centered at the origin. As a second point of reference, the second plot shows the results for an equivalent mass and volume system with the upwave and downwave floats separated from the center float by 20 m (and rigidly connected to the central float). The individual float dimensions were kept the same (Table 8) throughout. The remaining plots show the results for the floating Marson WEC with different separation distances. Out of all cases, the heave PTO with the floats centered performs the best. With the floats centered (rigidly connected together and to a heave PTO), all 3 experience in-phase wave excitation while the excitation may be slightly out of phase when the floats are separated, leading to lower power. When considering the cases with the rotational PTOs, they all perform relatively similarly. The 20 m separation distance performs best and generates more electrical power than the heave-only separated case but less power than the heave-only centered case. The comparison between the heaveonly and including rotational PTO cases are summarized on the left side of Figure 23 where the best performing gains were selected to maximize electrical power for each case.

It was expected that the addition of the floating WECs on either side of the central WEC could increase the total power capture. Whether simply the additional PTOs or the ability for the upwave and downwave floats (along with the effects of their control gains) to amplify the power capture of the heave PTO, it was believed that power would increase by including



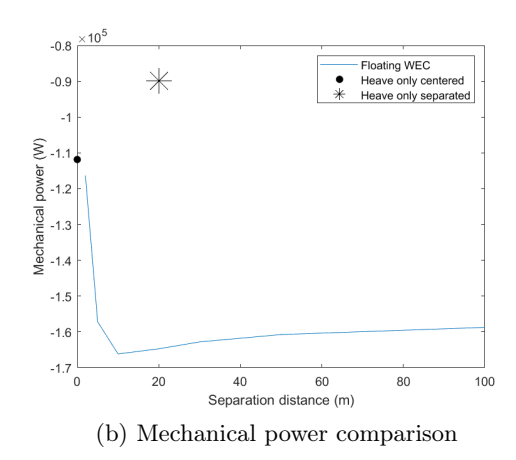


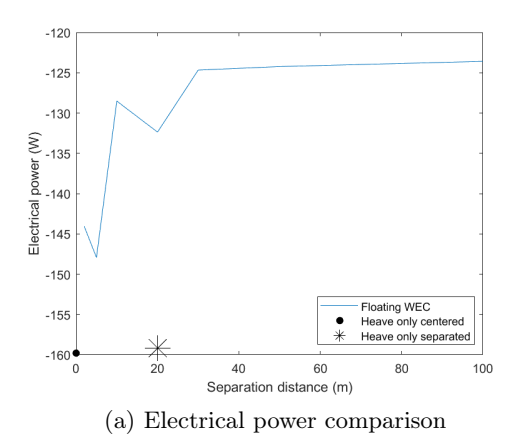
Figure 23: Comparison of floating WEC separation distances and heave-only cases in PacWave conditions.

the rotational PTOs. For example, the rotational PTOs could input power to the system to maximize power in the heave PTO in the WecOptTool analysis. On the other hand, the WEC-Sim models do not show this behavior. As shown on the left side of Figure 23, the heave-only case with the floats centered performs best no matter the separation distance.

One suspected reason for the lack of success of the WEC with rotational PTOs is that the PTOs (rotational PTOs assumed to have same parameters as heave PTOs) are not well designed for the setup and wave conditions. To remove some of the impact of PTO design, we can look at mechanical power (right side of Figure 23) instead of electrical power. The mechanical power shows significantly different results than the electrical power. The WEC including rotational PTOs consistently captures more mechanical power than either of the heave-only cases. Analyzing the PTOs in more detail, the heave PTO still dominates over the rotational PTOs in terms of power capture, but the additional dynamic inputs from the upwave and downwave floats and PTOs increase the power capture in the heave PTO significantly. With a 10 m separation distance, the floating Marson WEC is able to capture 16,600 W (mechanical power), a 49% improvement over the heave-only case in these seastates.

7.7.2 Great Lakes Conditions

While the improvements in electrical power performance with the floating WEC setup as compared to a heave-only PTO are minimal in PacWave conditions, the results may be different in smaller wave conditions. As suggested in Section 7.1, the wavelengths of interest for larger waves may be well above what are feasible separation distances for this design. Thus, testing shorter wavelength and height waves may yield more interesting results. A wave with a period of 3 s and height of 0.1 m was considered to represent conditions in the Great Lakes region of the United States. The grid of heave controller gains with the respective performance for the heave-only PTO cases and a range of separation distances is shown in Figure 32 in the Appendix and summarized in Figure 23). The results show the floating WEC with the best separation distance (5 m) still performs worse than the heave-only cases even in these small wave conditions. As with the PacWave conditions, the PTO parameters do not seem well designed for the rotational PTOs. When considering mechanical power however, the floating Marson WEC again outperforms the heave-only cases. For the 10 m separation



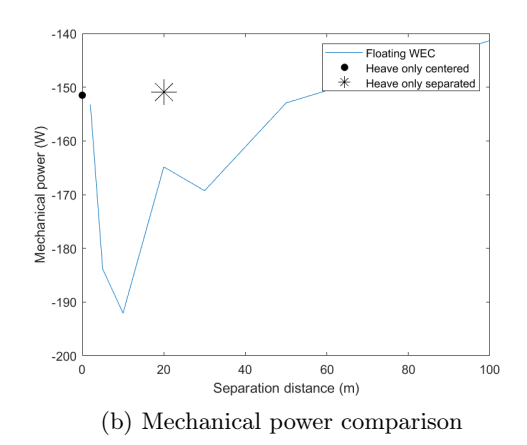


Figure 24: Comparison of floating WEC separation distances and heave-only cases in Great Lakes conditions.

distance, 192 W (mechanical power) is captured for a 27% increase over the heave-only cases.

7.8 Discussion and Conclusions

The Marson WEC design consists of multiple floats connected in series by rotational power take-off units. Two main configurations (floating and fixed-end shown in Figure 6) were analyzed throughout this project. First, WecOptTool's existing modeling techniques were challenging to adapt to the Marson WEC, and a system identification approach was used. The system ID was completed in WEC-Sim to identify the impedance and excitation transfer functions. These transfer functions were then input into WecOptTool. WecOptTool was used to optimize the controls and explore the relevant design space efficiently for the floating and fixed-end cases. While WecOptTool successfully explored the design space, the results were critically limited by the quality of the system ID. It is unclear the exact source of error (to be investigated further in future work), but the response and power modeled by WecOptTool was much larger than from equivalent WEC-Sim models. Some results and comparisons from the WecOptTool modeling still provided value in the design process but focus shifted to the WEC-Sim models for the end of the project to prioritize accuracy.

WEC-Sim is less efficient for design space exploration, making it difficult to model a comprehensive design space. Instead, a small number of important design variables were considered along with a comparison to a more traditional heave-only point absorber WEC. In discussions with the TSR, this was determined the most valuable next step: analyze the system to sufficiently determine if the Marson WEC design is worth pursuing further.

Through the confined design space exploration, the floating Marson WEC was found to perform worse than heave-only cases in terms of electrical power. On the other hand, the captured mechanical power of the Marson WEC was significantly greater (27 - 49% increase in mechanical power) than for the heave-only cases across different wave conditions. The power take-off and generator parameters were found to be very inefficient for the rotational PTOs. A better PTO design was outside the scope of this project but the mechanical power comparison shows the potential for the Marson WEC to outperform the heave-only cases.

To fully consider the Marson WEC and whether it is worth pursuing further, the costs need to be factored in alongside the power. A 49% improvement in power is significant, but if it doubles the WEC cost, it is simply not worth it. The floating Marson WEC would require

7.9 Lessons Learned 7 RESULTS

2 additional rotational PTOs as well as additional structural support for the lever arms when compared to a WEC with one float with the same mass and volume and only a heave PTO. Based on [10], the power take-off system comprises 24.2% of the WEC cost on average. As a very basic assumption, a tripling of the PTO cost could increase the total WEC cost by about 50%. Further considering the structural costs (38.2% of the WEC cost from [10]), it is certainly possible that the cost increases would exceed the 49% power increases. Additional floats and components would also decrease reliability.

WEC costs can be highly variable, and there are certainly other factors that have yet to be sufficiently resolved. These include the number of floats, PTO/generator parameters for the rotational PTOs, float shapes, etc. Fully resolving these factors as well as other considerations (such as hydraulic rotational PTOs that can store and input energy [11]) would help in better understanding the potential for the Marson WEC. Based on the analysis completed and WEC-Sim results, it is clear that the floating Marson WEC does have potential for success as a wave energy converter and is worth further investigation. Going forward, a key focus will be on assessing the balance between improving performance and additional costs/complexity.

7.9 Lessons Learned

As suggested above, there were a number of challenges encountered over the course of this award that have led to lessons applicable to future awards and related work. In summary:

- Challenges in BEM imply the scope was hugely inflated given the time and budget constraints: even automated, BEM batch runs of more than 2 to 3 bodies varying potentially in 3 dimensions, with varying spacing, the number of combinations even for a sparse parameter space quickly becomes untenable. Further, the stability of BEM results, and thus their suitability for use in WoT and WEC-Sim, become less reliable for large body numbers. While automated cleanup methods were employed (e.g. badBemioFixFcn.m in the wecSim distribution), this is only robust with manual review.
- The linearization of the kinematic linkage fundamental to the Marson device is not possible in the existing implementation of WecOptTool (although work is ongoing to resolve this). Similar WEC archetypes (attenuators, floating platform with relative pitch, etc.) will also be challenging to model in WecOptTool due to this limitation. This led to the reduction in scope, and the simplification of BEM results, the identification of impedance models in WEC-Sim: a much more time-consuming process. Greater consideration of this at the start with more proper go/no-go benchmarks could've helped conserve project funds.
- The system identification procedure struggled with the closely-coupled systems. Particularly with disparately sized floats, the actuation of one PTO would dominate the motions of others, resulting in a low signal to noise ratio on diagonal impedance elements even over excited frequencies. As a result, non-physical negative real parts were persistently estimated. A simple alternative procedure was pursued in which the diagonal elements were estimated in isolation, but its robustness is dubious as it assembles the impedance matrix in a piece-wise fashion: more robust procedures for close-coupled systems will be the subject of future investigations. In particular, it is believed that the system identification via matrix pseudo-inverse may struggle in cases where the excitation response matrices are not diagonally dominant.
- Even with the updated system identification procedure, the WecOptTool analysis resulted in controller gains that drove the system unstable in WEC-Sim. When gains

were adjusted for stability of the WEC-Sim model, the resultant electrical power was significantly smaller than from WecOptTool. While the controller gains were reasonable for the impedance models linearized around equilibrium, the WEC-Sim model fully models the nonlinear dynamic linkage (hinge locations are not stationary). It is believed that this key distinction (amplified for disparately sized floats) led to the differences in stability and performance between the WecOptTool and WEC-Sim model. This was unexpected, as similarly non-linear systems have seen success in this methodology in tank testing. Future work to resolve this specific issue would include a more detailed comparison between the WEC-Sim and WecOptTool impedance-based models in terms of responses and forces to identify the source of the problem. However, with the relatively small budget on TEAMER awards, a risk-averse (but less efficient) approach would be to run only WEC-Sim to analyze the system.

- The GBM approach to BEM modeling was not pursued because the continuous deflection would poorly approximate more sparsely placed floats: however, a GBM of a hinge type connection between two disparate floats (as a single mesh file) can now be modeled in Capytaine: for future awards, this single DOF system may be used to simplify broad parameter studies like this. A small challenge still would exist for translating the hydrostatics (mass and stiffness matrices) to the hinge degree of freedom but this does have a closed-form solution and could be trivially automated provided the kinematics are constrained to a suitably linear region. The single DOF results can facilitate impedance estimates in the PTO frame directly and can be used all the way until the WEC-Sim validation.
- Power take-off design is a key component of co-design. The PTO parameters were initially intended to be a central part of the design analysis, but challenges with model setup and identification led to scope reduction. Since the PTO parameters were assumed to be constant for most of the analysis, the results may be biased by the selected values.

8 CONCLUSIONS AND RECOMMENDATIONS

All told, there were a number of technical problems that precluded the completion of the proposed scope in a robust way. We have added this section to succinctly summarize findings and propose future work for the TSR and this WEC design.

- The floating Marson WEC seems to show the most promise. It may be especially useful in bi-modal seas (i.e., where swell and storm surge coexist), which commonly occur, if a cost-effective approach for the multiple PTOs can be determined.
- Given the dominance of the heave mode in power collection in realistic seas, it is unlikely that adding more floats in either configuration is a worthy area of study.
- Efficient PTO design/selection is vital to a well-performing WEC and careful consideration will need to be made for future PTO design analysis, factoring in tradeoffs between component ratings, losses, and costs and likely unique parameters for the different PTOs in the system.
- The struggles with system identification for the low-impedance kinematic chain (one-end-fixed) and the strongly coupled (free-floating) WECs are recommended as example

BIBLIOGRAPHY BIBLIOGRAPHY

cases for refinement of these techniques: these are the simplest WEC geometries investigated to date for which these difficulties were severe enough to prevent further co-design steps.

BIBLIOGRAPHY

- [1] R. G. Coe, G. Bacelli, S. J. Spencer, and D. Forbush, "Advanced wec dynamics and controls mask3 test," 2019.
- [2] R. G. Coe, G. Bacelli, and D. Forbush, "A practical approach to wave energy modeling and control," *Renewable and Sustainable Energy Reviews*, vol. 142, p. 110791, 2021. [Online]. Available: https://doi.org/10.1016/j.rser.2021.110791
- [3] C. A. Strofer, D. T. Gaebele, R. G. Coe, and G. Bacelli, "Control co-design of power take-off systems for wave energy converters using wecopttool," *IEEE Transactions on Sustainable Energy*, 10 2023.
- [4] G. Bacelli, R. G. Coe, D. Patterson, and D. Wilson, "System identification of a heaving point absorber: Design of experiment and device modeling," *Energies*, vol. 10, 4 2017.
- [5] R. G. Coe, G. Bacelli, S. Olson, V. S. Neary, and M. B. Topper, "Initial conceptual demonstration of control co-design for wec optimization," *Journal of Ocean Engineering and Marine Energy*, vol. 6, pp. 441–449, 2020. [Online]. Available: https://doi.org/10.1007/s40722-020-00181-9
- [6] M. Ancellin and F. Dias, "Capytaine: a python-based linear potential flow solver," *Journal of Open Source Software*, vol. 4, p. 1341, 2019.
- [7] N. Tom, K. Ruehl, A. Keester, D. Ogden, D. Forbush, S. Husain, J. Leon, J. Grasberger, M. Topper, and Y.-H. Yu, "New developments and capabilities within wec-sim: Preprint," 2023. [Online]. Available: www.nrel.gov/publications.
- [8] R. G. Coe, G. Bacelli, D. Forbush, S. J. Spencer, K. J. Dullea, B. Bosma, and P. Lomonaco, "Foswec dynamics and controls test report," Sandia National Lab.(SNL-NM), Albuquerque, NM (United States), Tech. Rep., 2020.
- [9] C. A. M. Ströfer, D. T. Gaebele, R. G. Coe, and G. Bacelli, "Control co-design of power take-off systems for wave energy converters using wecopttool," *IEEE Transactions on Sustainable Energy*, vol. 14, no. 4, pp. 2157–2167, 2023.
- [10] C. Guo, W. Sheng, D. G. De Silva, and G. Aggidis, "A review of the levelized cost of wave energy based on a techno-economic model," *Energies*, vol. 16, no. 5, p. 2144, 2023.
- [11] J. A. Leon-Quiroga, D. Ogden, S. Husain, W. Sheng, G. Aggidis, and A. Bharath, "Design and performance evaluation of a resistive control using a hydraulic pto system for the talos wave energy converter," in *ISOPE International Ocean and Polar Engineering Conference*. ISOPE, 2024, pp. ISOPE–I.

9 ACKNOWLEDGMENTS

Sandia National Laboratories is a multi-mission laboratory managed and operated by National Technology and Engineering Solutions of Sandia, LLC., a wholly owned subsidiary of Honeywell International, Inc., for the U.S. Department of Energy's National Nuclear Security Administration under contract DE-NA0003525. This paper describes objective technical results and analysis. Any subjective views or opinions that might be expressed in the paper do not necessarily represent the views of the U.S. Department of Energy or the United States Government.

10 APPENDIX

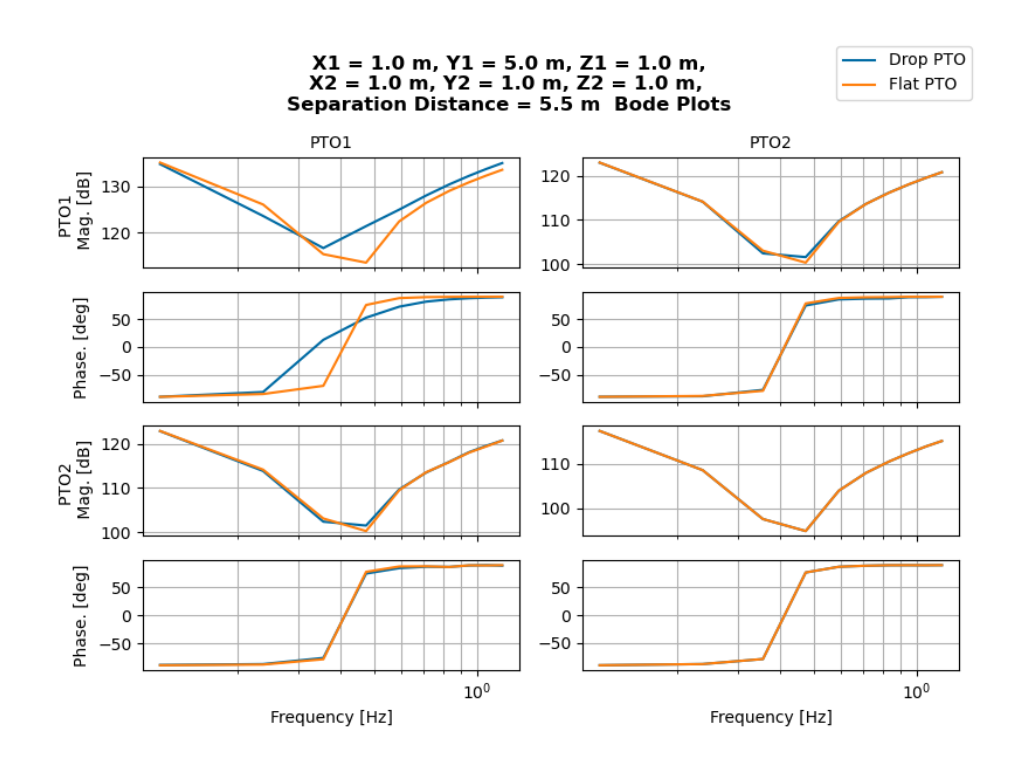


Figure 25: Interpolated impedance for count 4 with both drop and flat PTOs.

Table 9: Tested dimensions for fixed-end WEC configuration. Each count was also tested for multiple iterations: a drop and a flat PTO and a Z dimension of 1 m and 5 m. All dimensions are in m. The first PTO was located at the origin with the second PTO located at the center of the float in the x-direction.

| | Float 1 | | | | Float 2 | | | |
|-------|---------|----|--------------|-------|---------|----|--------------|-------|
| Count | X | Y | \mathbf{Z} | X loc | X | Y | \mathbf{Z} | X loc |
| 1 | 1 | 1 | 1 / 5 | -1 | 1 | 1 | 1 / 5 | -2.5 |
| 2 | 1 | 1 | 1 / 5 | -5 | 1 | 1 | 1 / 5 | -10.5 |
| 3 | 1 | 5 | 1 / 5 | -1 | 1 | 1 | 1 / 5 | -2.5 |
| 4 | 1 | 5 | 1 / 5 | -5 | 1 | 1 | 1 / 5 | -10.5 |
| 5 | 1 | 1 | 1 / 5 | -1 | 1 | 5 | 1 / 5 | -2.5 |
| 6 | 1 | 1 | 1 / 5 | -5 | 1 | 5 | 1 / 5 | -10.5 |
| 7 | 1 | 5 | 1 / 5 | -1 | 1 | 5 | 1 / 5 | -2.5 |
| 8 | 1 | 5 | 1 / 5 | -5 | 1 | 5 | 1 / 5 | -10.5 |
| 9 | 1 | 15 | 1 / 5 | -1 | 1 | 1 | 1 / 5 | -2.5 |
| 10 | 1 | 15 | 1 / 5 | -5 | 1 | 1 | 1 / 5 | -10.5 |
| 11 | 1 | 1 | 1 / 5 | -1 | 1 | 15 | 1 / 5 | -2.5 |
| 12 | 1 | 1 | 1/5 | -5 | 1 | 15 | 1 / 5 | -10.5 |
| 13 | 1 | 15 | 1 / 5 | -1 | 1 | 15 | 1 / 5 | -2.5 |
| 14 | 1 | 15 | 1 / 5 | -5 | 1 | 15 | 1 / 5 | -10.5 |
| 15 | 5 | 1 | 1 / 5 | -5 | 1 | 1 | 1 / 5 | -8.5 |
| 16 | 5 | 1 | 1 / 5 | -25 | 1 | 1 | 1 / 5 | -32.5 |
| 17 | 1 | 1 | 1 / 5 | -1 | 5 | 1 | 1 / 5 | -6.5 |
| 18 | 1 | 1 | 1 / 5 | -5 | 5 | 1 | 1 / 5 | -30.5 |
| 19 | 5 | 1 | 1 / 5 | -5 | 5 | 1 | 1 / 5 | -12.5 |
| 20 | 5 | 1 | 1 / 5 | -25 | 5 | 1 | 1 / 5 | -52.5 |
| 21 | 5 | 5 | 1 / 5 | -5 | 1 | 1 | 1 / 5 | -8.5 |
| 22 | 5 | 5 | 1 / 5 | -25 | 1 | 1 | 1 / 5 | -32.5 |
| 23 | 1 | 1 | 1 / 5 | -1 | 5 | 5 | 1 / 5 | -6.5 |
| 24 | 1 | 1 | 1 / 5 | -5 | 5 | 5 | 1 / 5 | -30.5 |
| 25 | 5 | 5 | 1/5 | -5 | 5 | 5 | 1 / 5 | -12.5 |
| 26 | 5 | 5 | 1 / 5 | -25 | 5 | 5 | 1 / 5 | -52.5 |
| 27 | 5 | 15 | 1 / 5 | -5 | 1 | 1 | 1 / 5 | -8.5 |
| 28 | 5 | 15 | 1 / 5 | -25 | 1 | 1 | 1 / 5 | -32.5 |
| 29 | 1 | 1 | 1 / 5 | -1 | 5 | 15 | 1 / 5 | -6.5 |
| 30 | 1 | 1 | 1 / 5 | -5 | 5 | 15 | 1 / 5 | -30.5 |
| 31 | 5 | 15 | 1 / 5 | -5 | 5 | 15 | 1 / 5 | -12.5 |
| 32 | 5 | 15 | 1/5 | -25 | 5 | 15 | 1 / 5 | -52.5 |
| 33 | 5 | 15 | 1 / 5 | -5 | 1 | 5 | 1 / 5 | -8.5 |
| 34 | 5 | 15 | 1 / 5 | -25 | 1 | 5 | 1 / 5 | -32.5 |
| 35 | 1 | 5 | 1/5 | -1 | 5 | 15 | 1 / 5 | -6.5 |
| 36 | 1 | 5 | 1 / 5 | -5 | 5 | 15 | 1 / 5 | -30.5 |

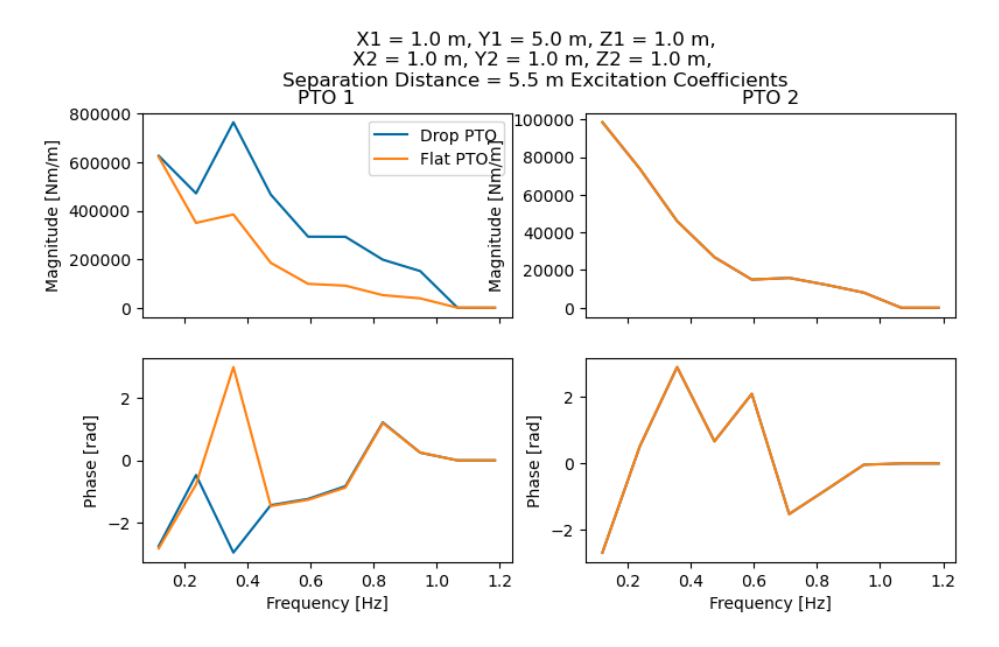


Figure 26: Interpolated excitation for count 4 with both drop and flat PTOs.

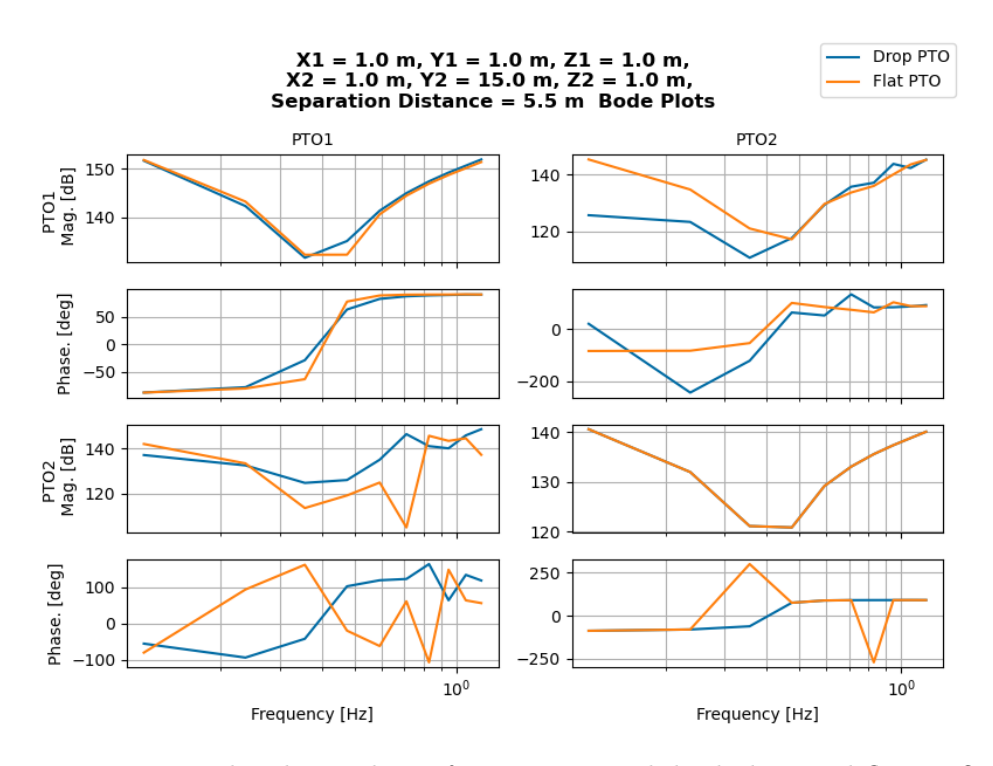


Figure 27: Interpolated impedance for count 12 with both drop and flat PTOs.

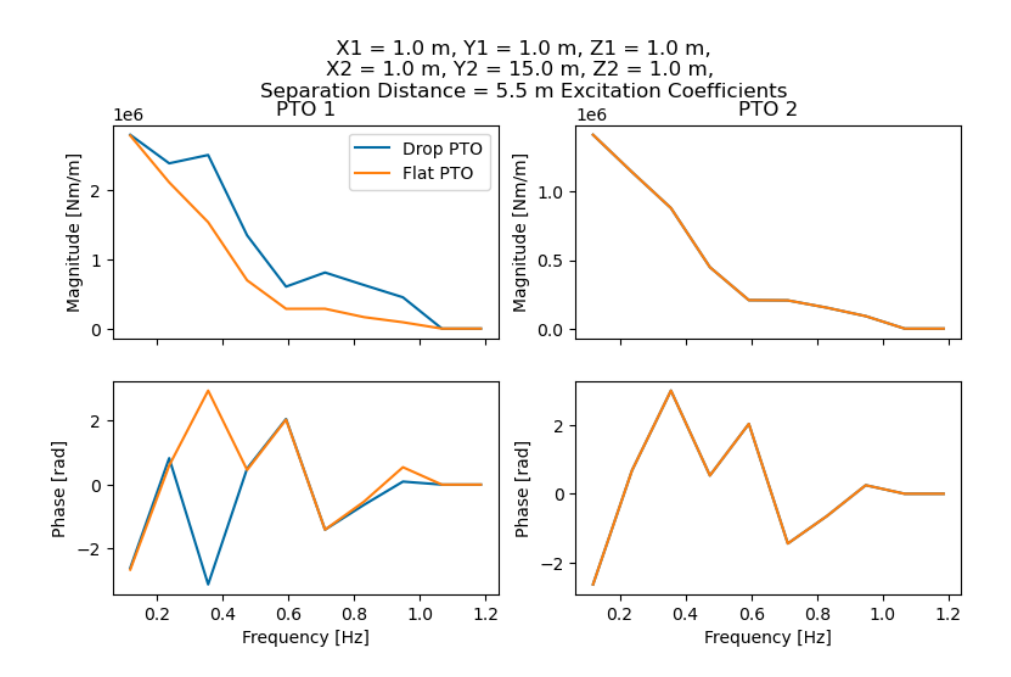


Figure 28: Interpolated excitation for count 12 with both drop and flat PTOs.

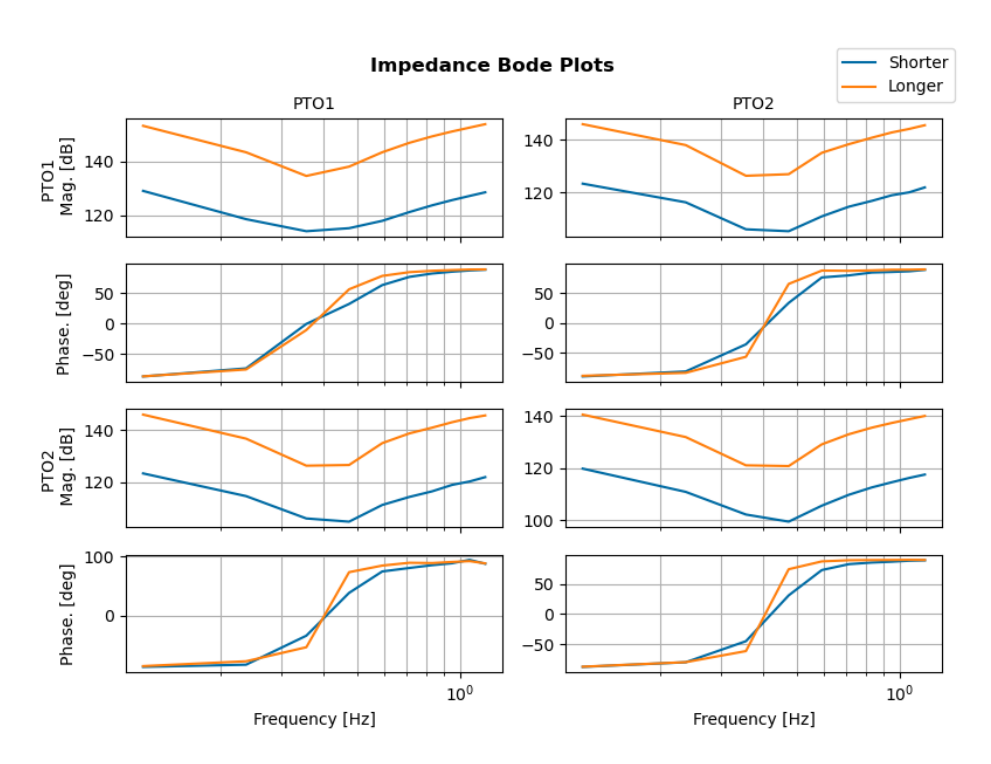


Figure 29: Interpolated impedance comparing shorter to longer float separation distances.

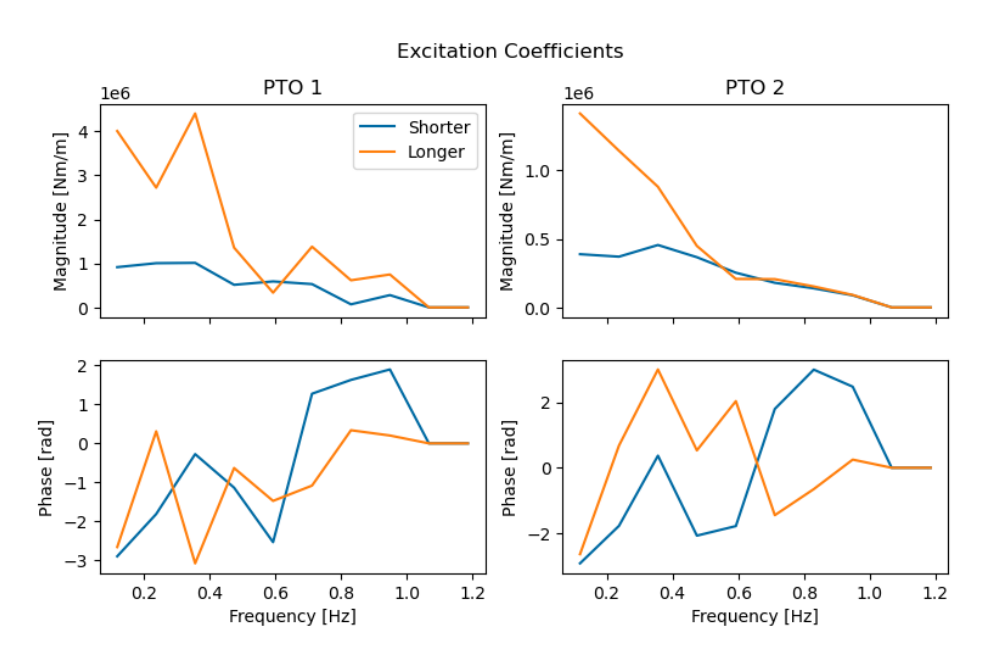


Figure 30: Interpolated excitation comparing shorter to longer float separation distances.

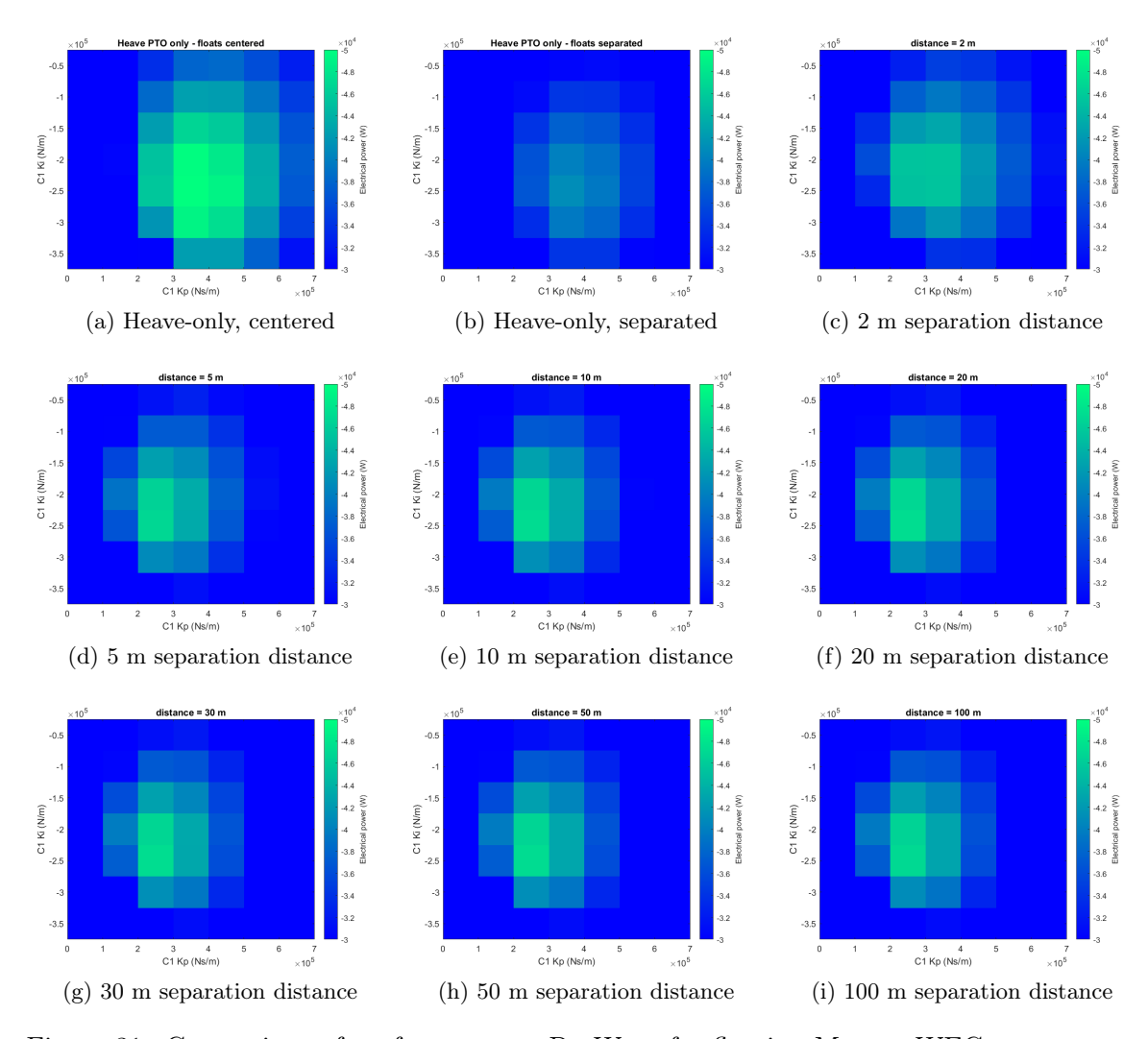


Figure 31: Comparison of performance at PacWave for floating Marson WEC arrangement with heave, upwave, and downwave PTOs of various separation distances versus a heave-only WEC centered or separated.

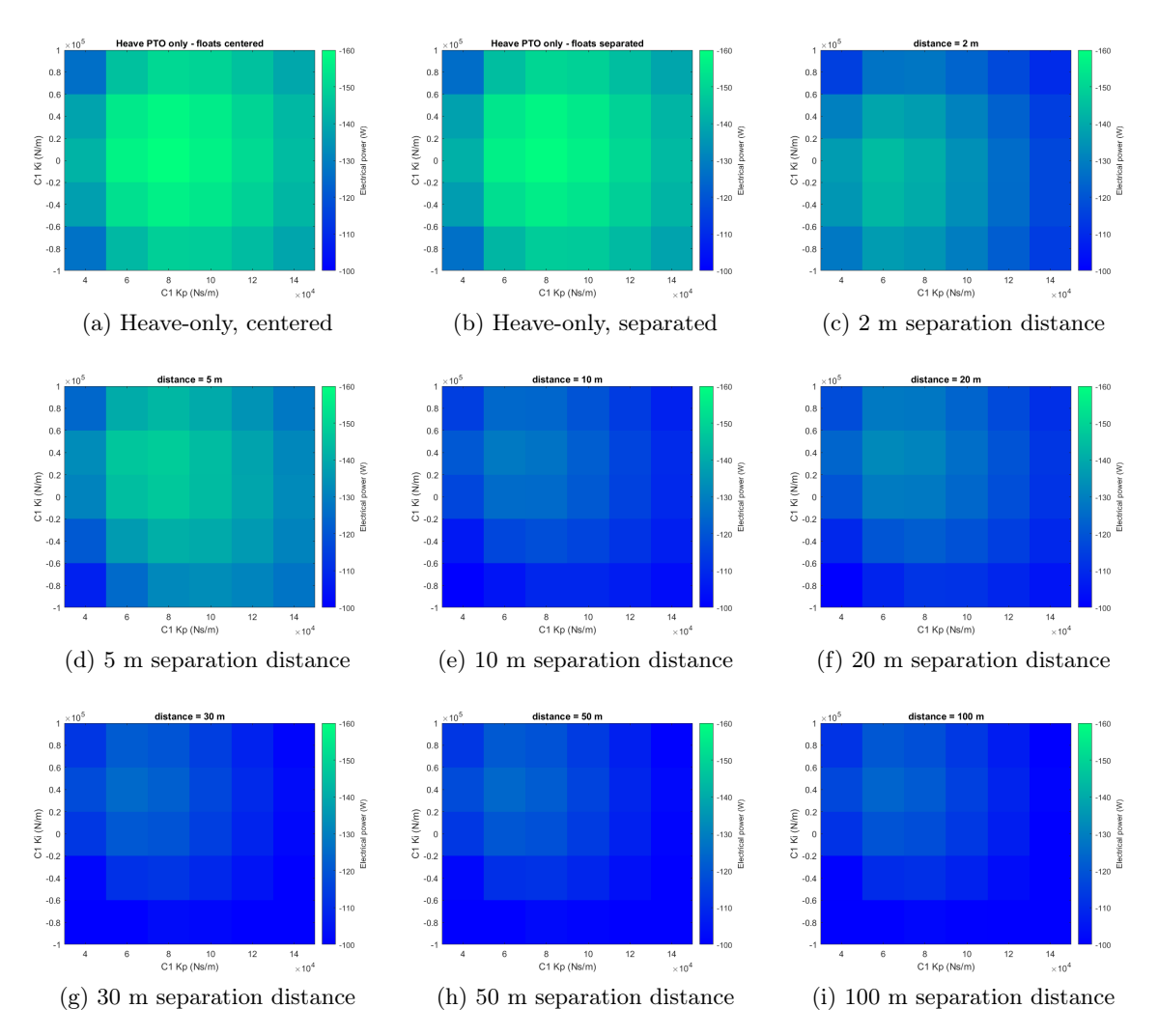


Figure 32: Comparison of performance in Great Lakes conditions for floating Marson WEC arrangement with heave, upwave, and downwave PTOs of various separation distances versus a heave-only WEC centered or separated.